2025-01-17

Oxygen Isotope Dynamics of Lake Water and Dissolved Phosphate in Saline Lakes of the Cariboo Plateau of British Columbia, Canada

Walters, Liam

UNIVERSITY OF CALGARY

Oxygen Isotope Dynamics of Lake Water and Dissolved Phosphate in Saline Lakes of the Cariboo Plateau of British Columbia, Canada

by

Liam Walters

A THESIS

SUBMITTED TO THE FACULTY OF GRADUATE STUDIES

IN PARTIAL FULFILMENT OF THE REQUIREMENTS FOR THE

DEGREE OF MASTER OF SCIENCE

GRADUATE PROGRAM IN GEOSCIENCE

CALGARY, ALBERTA

JANUARY, 2025

Abstract

Phosphate availability is a critical constraint on prebiotic chemistry, yet natural environments rarely achieve concentrations compatible with origin-of-life experiments. Alkaline and saline lakes have emerged as potential solutions to this "phosphate problem," but the mechanisms controlling phosphate cycling in these extreme environments remain poorly understood. Here, I investigate phosphate dynamics in the alkaline Last Chance and Goodenough Lakes and the magnesium sulfate-rich Basque Lakes of British Columbia's Interior Plateau using oxygen isotope analysis of dissolved phosphate ($\delta^{18}O_{PO_4}$) and lake waters ($\delta^{18}O_{H_2O}$). I developed a modified silver phosphate precipitation protocol to enable isotopic analysis of phosphate in these chemically extreme waters. My results show that Last Chance Lake maintains phosphate concentrations up to 12 mmol/L through primarily abiotic processes, evidenced by significant deviations (up to +5.3 ‰) from oxygen isotopic equilibrium (denoted $\Delta\delta^{18}O_{PO_4}$). However, neighboring Goodenough Lake's extensive microbial mats drive near-equilibrium signatures ($\Delta\delta^{18}O_{PO_4} \approx$ +2.2 ‰) while limiting phosphate accumulation. In contrast, my analysis of the Basque Lakes demonstrates how extreme brine chemistry can maintain phosphate far from equilibrium ($\Delta\delta^{18}O_{PO_4}$ up to +10.7 ‰) through abiotic processes such as adsorption and phosphate mineral precipitation. These findings validate theoretical predictions of phosphate concentration mechanisms in alkaline environments and provide a framework for interpreting potential biosignatures in ancient Earth settings and extraterrestrial environments.

Acknowledgments

First and foremost, I would like to acknowledge the generous funding support from the Natural Sciences and Engineering Research Council of Canada (NSERC) and the Canadian Government that made this research possible. I am grateful to the University of Calgary and the Department of Earth, Energy, and Environment for providing the resources, facilities, and supportive environment essential for completing this work.

I extend my deepest gratitude to my supervisor, Dr. Benjamin Tutolo, whose expertise, unwavering patience, and open-door policy have been instrumental in my development as a researcher. His guidance and support throughout this journey have been invaluable.

Special thanks to Dr. Christopher Tino for his endless patience in answering my near-hourly questions and for his invaluable assistance in developing innovative approaches for removing chloride during the silver phosphate precipitation process. I am particularly grateful to Serhat Sevgen for the enlightening late-night discussions and his crucial contribution in performing phosphorus concentration analysis using Gallery. I would like to thank Cameron Wood for his expertise and guidance in getting me started in the laboratory, particularly regarding the phosphate isolation and silver phosphate precipitation procedures. The previous work of Shane Bossaer in collecting data on these lakes is much appreciated.

I would also like to express my gratitude to Dr. Veith Becker and the Isotope Science Lab for conducting the stable isotope analyses of water and generously allowing me to use their facilities for Ag_3PO_4 packaging. Additionally, I extend my sincere thanks to Dr. Laszlo Kocsis and The Stable Isotope Laboratory at the University of Lausanne for their work in analyzing $\delta^{18}O_{PO_4}$.

Finally, I would like to thank my parents, Mark and Ziva, for their constant support and encouragement throughout this journey.

This work represents not just my own efforts, but the collective support and guidance of many individuals who have contributed to its completion.

Table of Contents

List of Tables

List of Figures

1. Introduction

1.1 Prebiotic Chemistry and the Origin of Life

The origins of life have intrigued scientists for centuries, beginning with Charles Darwin's suggestion of a "warm little pond," where simple chemicals, influenced by heat, light, and other forces, might combine to form life's precursors (Darwin 1859). This concept laid a foundation for understanding life's emergence in confined, nutrient-rich environments, where organic molecules could assemble and potentially give rise to early cellular structures. Building on Darwin's ideas, Alexander Butlerow's work in 1861 demonstrated that simple carbon compounds could react to form complex molecules like sugars under controlled conditions, establishing the concept of chemical synthesis (Butlerow 1861). Butlerow's experiments reinforced the notion that life's building blocks could form naturally, providing a basis for prebiotic chemistry.

A key emphasis within the origin-of-life literature is the availability and biological incorporation of phosphorus. This foundation was expanded by Joan Oró's studies in the 1960s, which provided direct experimental evidence that molecules essential to life, such as adenine, could form under early Earth conditions. Oró demonstrated that nucleotides could be synthesized from hydrogen cyanide, an abundant molecule on prebiotic Earth, supporting Darwin's hypothesis by showing how life's foundational molecules might self-assemble in plausible prebiotic environments (Oró 1961). Darwin's "warm little pond" hypothesis finds modern parallels in contemporary saline lakes, which, with their mineral-rich environments and cyclic wet-dry conditions, may resemble the early Earth scenarios critical to prebiotic chemistry (Powner et al. 2009; Becker et al. 2018).

Previous research has highlighted how phosphate, critical for nucleic acid backbones and cellular structures, likely accumulated in these lakes through wet-dry cycles and mineral interactions, aiding complex molecule formation (Deamer et al. 2006; Patel et al. 2015). Recent studies have specifically identified saline lakes with high alkalinity (herein referred to as alkaline lakes) as potential modern analogues for environments that may have hosted the first lifeforms (Toner and Catling 2019, 2020; Liu et al. 2020). These environments exhibit fluctuating conditions and natural cycles of evaporation and hydration, creating settings that could facilitate the concentration and interaction of organic molecules (Hurowitz et al. 2023). In sum, these studies reveal that alkaline conditions could drive the synthesis of essential prebiotic compounds by concentrating and stabilizing reactants in shallow, evaporative settings.

1.2 Phosphorus as an Essential Element

Phosphorus (P), the 11th most abundant element on Earth, comprises approximately 0.09 % of the Earth's crust and predominantly exists in the form of phosphate minerals such as apatite and vivianite (Filippelli 2008). Through weathering, P is gradually liberated from these minerals, entering soils and aquatic systems where it undergoes continuous cycling via biological and geological processes (Cole et al. 1977). Interestingly, Martian rocks have shown P concentrations roughly twice that of Earth's crust, and in more recent years it has been found that Mars is approximately 8 times richer in phosphate than Earth (Greenwood and Blake 2006; Hausrath et al. 2024).

In terrestrial ecosystems, P is ubiquitous across all domains of life due to its fundamental role in a wide range of biological molecules. Within nucleic acids like DNA and RNA, phosphate groups link nucleotides together, creating the backbone necessary for storing and transmitting genetic information (Westheimer 1987). Furthermore, P is essential in cellular membranes, where it exists as part of phospholipids, contributing to membrane integrity and regulating molecular transport in and out of cells (Lécuyer et al. 1999). Beyond structural functions, P is also central to metabolic energy transfer through adenosine triphosphate (ATP), which, upon hydrolysis, releases energy critical to cellular processes by converting ATP to adenosine diphosphate (ADP) and inorganic phosphate (P_i) (Dittrich et al. 2003). The ATP hydrolysis reaction, expressed as $ATP + H_2O \rightarrow ADP + P_i$, is fundamental to cellular energy dynamics and mediated by the enzyme ATPase (Elghobashi-Meinhardt 2024).

The stability of the phosphate ion (PO_4^{3-}) further enhances its utility within biological structures and processes. The phosphorus-oxygen (P-O) bonds in phosphate have partial double-bond character due to resonance, which delocalizes negative charge across the oxygen atoms, reducing electron repulsion and enhancing bond strength (Westheimer 1987; Berg et al. 2010). The distribution of the negative charge also acts as a defense mechanism against hydrolysis by nucleophiles, such as hydroxide ions, a mechanism vitally important in the stability and persistence of genetic material (Westheimer 1987). This stability allows phosphate compounds to remain intact under typical environmental conditions, a key factor in the persistence of biomolecules like DNA and RNA. However, to enable phosphate cycling and metabolic processes, these stable P-O bonds

are cleaved by specific enzymes, such as phosphatases and pyrophosphates, facilitating biological P turnover (Blake et al. 2005).

1.3 Alkaline and Saline Lakes as a Solution to the Phosphate Problem

Phosphate is indispensable in prebiotic chemistry, serving as a backbone for nucleic acids and playing a pivotal role in energy transfer through molecules like ATP (Powner et al. 2009). However, the "phosphate problem" arises from the low solubility and availability of phosphate in natural aqueous environments, posing a challenge for prebiotic synthesis (Schwartz 2006; Toner and Catling 2020). The core of the problem is that phosphate concentrations in the natural environment are typically much lower than those needed to facilitate useful prebiotic experiments. For instance, a typical natural environment has ~10^{-6} M phosphate, versus the ~0.1–1 M concentrations used in prebiotic nucleotide-forming phosphorylation experiments (Hudson et al. 2000; Powner et al. 2009; Morasch et al. 2019; Xu et al. 2019; Toner and Catling 2020). This scarcity arises from phosphorus' relatively low crustal abundance coupled with its strong affinity to bind with cations such as calcium, leading to the formation of insoluble mineral compounds like apatite (Elser and Haygarth 2021). This geochemical behavior often results in phosphorus being the limiting nutrient in most environments, including the ocean throughout extended intervals of geologic time (Ruttenberg 2014; Reinhard et al. 2017).

Toner and Catling (2020) proposed that carbonate-rich lakes could offer a solution to the phosphate problem by facilitating the precipitation of calcium as carbonate minerals, such as dolomite, instead of apatite. In these environments, high concentrations of carbonate ions promote the formation of calcium carbonate minerals (e.g., calcite or dolomite) via:

$$Ca^{2+} + CO_3^{2-} \rightleftharpoons CaCO_3 \quad (1)$$

which sequesters calcium into the sediments and limits Ca^{2+} concentrations in solution. The resultant, low Ca^{2+} concentrations increase PO_4^{3-} solubility via, e.g.:

$$\text{Hydroxyapatite} + H^+ \rightleftharpoons 5\ Ca^{2+} + 3\ PO_4^{3-} + H_2O \quad (2)$$

The resultant, increased solubility of apatite (the hydroxyapatite end member in this case) allows phosphate to remain dissolved in the water at concentrations conducive to prebiotic chemical reactions (Fig. 1; Tutolo et al. 2024).

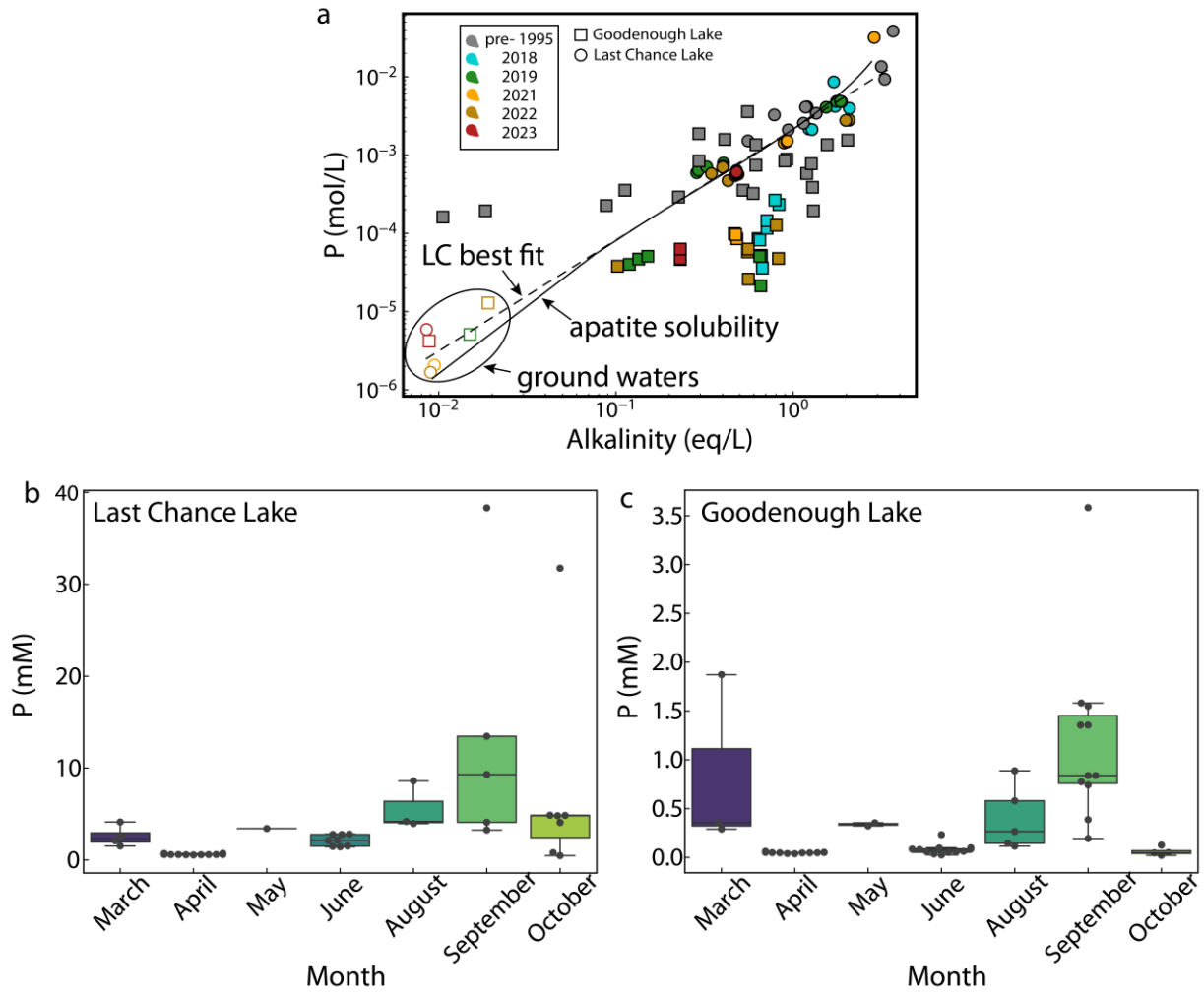

Figure 1: (a) The groundwater-lake water divide in alkaline lake systems. Phosphorus (P) and alkalinity measured in Last Chance and Goodenough Lake and groundwaters between 1991 and 2023. The dashed line is fit to the post-2018 Last Chance Lake data measured in this study, while the solid line represents calculated apatite solubility. The close agreement indicates apatite solubility likely controls total P concentration. (b) and (c) illustrate monthly variation in P concentration (mM). Figure from Tutolo et al. (2024).

Building on this concept, investigations of Last Chance Lake, an alkaline lake in the Cariboo Plateau of western Canada, indicate it is the world's most phosphate-rich lake, with concentrations reaching up to 37 mM (Hirst 1995; Toner and Catling 2020; Haas et al. 2024). These findings

provide evidence that experimental observations of phosphate-catalyzed synthesis of ribonucleotides, crucial for the construction of early genetic material (Powner et al. 2009; Patel et al. 2015; Cohen et al. 2024), could occur under plausible natural conditions.

Alkaline and saline lakes are unique geological formations characterized by high pH levels and salinity, resulting from closed-basin structures and intense evaporation processes in arid or semi-arid regions (Eugster and Hardie 1978; Rosen 1994; Williams 1996; Tutolo and Tosca 2023). These lakes accumulate dissolved ions over time, as limited outflow means that inflowing freshwater deposits minerals that stay as water evaporates, concentrating salts and increasing alkalinity (Jenkins 1918; Bern et al. 2021; Tosca and Tutolo 2023). High concentrations of carbonate and bicarbonate ions buffer the water's pH, making these lakes chemically stable and highly alkaline (Pecoraino et al. 2015; Chase et al. 2021; Mouginis-Mark and Wilson 2022). Seasonal evaporation cycles further enhance mineral saturation, promoting the precipitation of evaporite minerals such as halite, gypsum, and trona, which contribute to the lakes' mineralogy (Jenkins 1918; Eugster and Hardie 1978; Raudsepp et al. 2023). The elevated ionic strength in these waters support diverse geochemical conditions that parallel hypothesized early Earth environments, offering insights into ancient closed-basin chemistry and potential prebiotic settings (Williams 1996; Toner and Catling 2019; Haines et al. 2023).

Modern alkaline and saline lakes owe much of their distinctive chemistry to ongoing water-rock interactions, particularly with volcanic or basaltic substrates. These interactions release a range of ions into the water, including sodium, calcium, magnesium, silica, and carbonate, which contribute to the geochemical profiles of these lakes (Pecoraino et al. 2015; Chase et al. 2021; Raudsepp et al. 2023). The high concentrations of sodium, carbonate, and bicarbonate ions produced from these interactions play a critical role in maintaining the lake's high pH, stabilizing the environment against pH fluctuations and providing chemical conditions favorable for preserving organic compounds (Toner and Catling 2019; Tosca and Tutolo 2023). Evaporation of the waters causes them to exceed calcium carbonate solubility constraints, which, in turn, limits Ca^{2+} concentrations and permits increases in phosphate concentrations according to Reactions 1 and 2. This mineral precipitation also influences the sedimentary makeup of the lakebed, creating distinct layers of minerals that record chemical changes over time, with indications of concentrations of important elements such as P in the lake waters that deposited them (Ingalls et al. 2020).

These geochemical processes offer a model for understanding ancient lakes on early Earth, where similar conditions likely prevailed due to abundant volcanic activity, basaltic crust, and the absence of complex biological processes that would otherwise alter the chemical landscape (Eugster and Hardie 1978; Mouginis-Mark and Wilson 2022). During the Hadean and Archean eons, closed-basin lakes may have formed on volcanic islands that emerged above water (Rosas and Korenaga 2021), where water-rock interactions increased alkalinity and stabilized high pH environments. These conditions would have been crucial for facilitating prebiotic chemical reactions, as the buffering system mitigates drastic environmental changes and could limit the constant exposure to water through evaporative cycles and solute concentration (Williams 1996; Michael Marshall 2020; Haines et al. 2023).

Extending the search for life beyond Earth, Hausrath et al. (2024) investigated ancient Martian lake deposits for signs of elevated P concentrations. Their research analyzed Martian meteorites, identifying phosphate minerals indicative of past aqueous activity (Hausrath et al. 2024). These findings suggest that ancient Martian lakes may have had the necessary P levels to support prebiotic chemistry, offering insights into the planet's potential habitability. Moreover, chemical measurements performed by the *Curiosity* rover at the Groken site in Gale Crater show evidence for P mobility and deposition as, potentially, Mn,Fe-phosphate minerals (Treiman et al. 2023). The mineralogy of these Martian lake deposits are thought to have formed via processes similar to the evaporative conditions that concentrate P on Earth (Hurowitz et al. 2023). Further out in the solar system, analyses of the Saturnian moon Enceladus' cryovolcanic plumes have revealed that its subsurface ocean contains orthophosphate concentrations at least 100 times higher than those found in Earth's oceans, attributed to the higher solubility of calcium phosphate minerals in moderately alkaline, carbonate-rich environments, an environment potentially analogous to alkaline, saline lakes on Earth (Hao et al. 2022; Postberg et al. 2023).

Collectively, these studies point to the significance of specific environmental conditions—such as high alkalinity, wet-dry cycles, and the presence of calcium carbonate minerals—in concentrating P to levels that could facilitate the emergence of life (Toner and Catling 2020). By examining both terrestrial analogues and extraterrestrial environments with the aim of better understanding plausible chemical milieus for the origin-of-life, we can continue to unravel the mysteries behind the start of our biosphere and the potential for life elsewhere in the universe.

1.4 Intermontane British Columbia Lakes as Analogues for Origin-of-Life Environments

The alkaline and saline lakes of the Interior Plateau in British Columbia, Canada, exemplify modern settings where water-rock interactions and extreme geochemical conditions may mirror those of hypothesized early Earth lakes. As closed-basin systems, these lakes accumulate salts through seasonal cycles of evaporation, leading to the formation of dense brines and mineral-rich environments that resemble ancient lake systems in chemical composition (Jones et al. 2009).

The lakes studied in this thesis belong to two distinct closed-basin types within the region. The first group comprises the alkaline lakes of the Cariboo Plateau, including Last Chance and Goodenough Lakes, which exhibit high carbonate alkalinity, high pH, significant phosphate concentrations, and interactions with basaltic bedrock. These lakes serve as natural laboratories for studying abiotic and biologically mediated phosphorus cycling in high-alkalinity settings. The second group includes the saline, magnesium-sulfate-rich Basque Lakes, located in the Thompson Plateau and overlying the Cache Creek Terrane. These lakes provide an opportunity to study extreme brine chemistry and mineral precipitation processes, offering analogues for environments on Mars and other extraterrestrial settings.

Together, these lakes present contrasting examples of closed-basin systems shaped by differing geology, hydrology, and climatic conditions. They provide valuable insight into the geochemical and biogeochemical processes that may have influenced prebiotic chemistry and the origins of life on early Earth.

1.4.1 Last Chance and Goodenough Lakes Environment

The alkaline lakes of the Cariboo Plateau, including Last Chance and Goodenough Lakes (Fig. 2), exemplify high-pH, closed-basin systems shaped by interactions between basaltic bedrock, limited drainage, and the semi-arid climate of British Columbia's southern interior. These lakes serve as natural laboratories for studying water-rock interactions and the effects of extreme alkalinity and salinity on nutrient cycling and mineral formation. While both lakes are characterized by high-alkalinity waters, they are geochemically and biologically distinct, offering complementary

frameworks for understanding phosphorus cycling in early Earth-like conditions (Toner and Catling 2020; Haas et al. 2024).

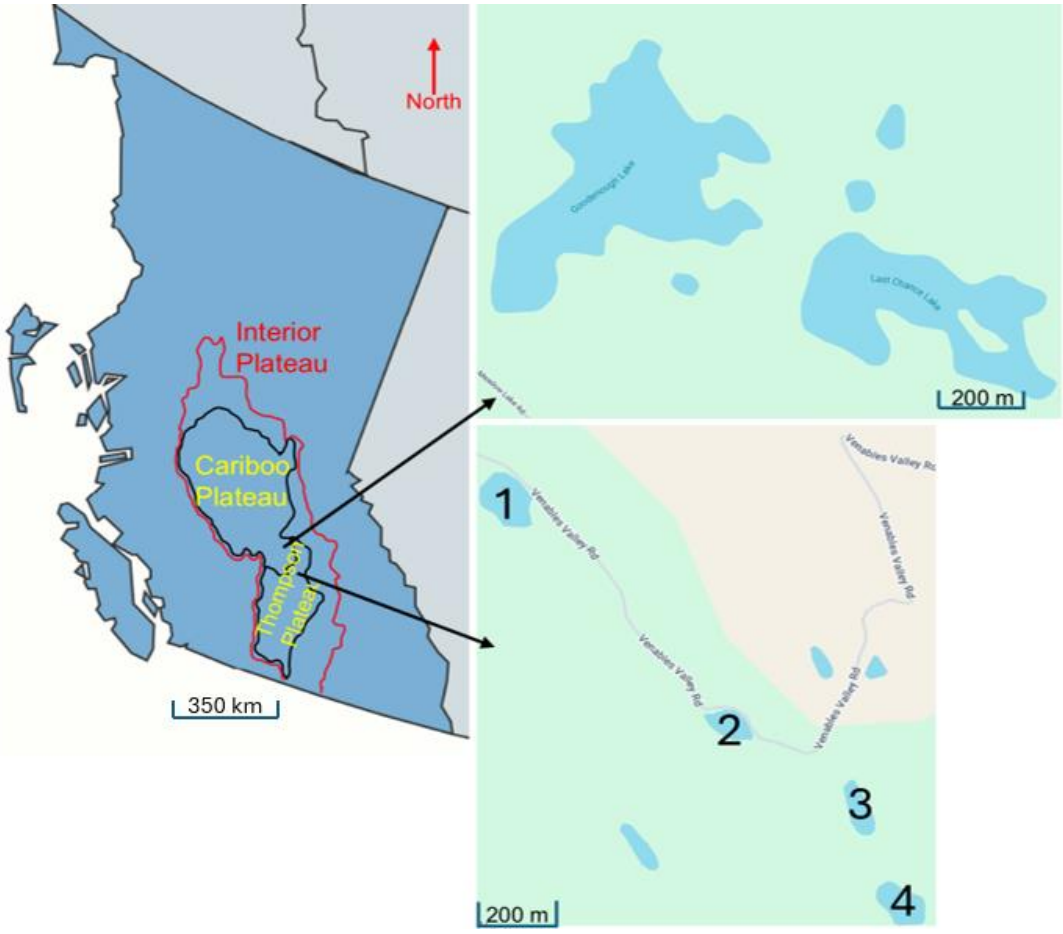

Figure 2: Map of British Columbia (BC) showing the Cariboo and Thompson Plateaus outlined within the broader Interior Plateau, which is geographically bounded by the Cascade Mountains to the east and the Coast Mountains to the west. Insets include a map of Last Chance and Goodenough Lakes (top) and a map of the Basque Lakes system, numbered 1 through 4 (bottom).

The Cariboo Plateau, part of the larger Fraser Plateau, lies within the semi-arid southern interior of British Columbia, Canada, and extends from Quesnel in the north to Clinton in the south (Campbell and Tipper 1971; Hirst 1995). Bounded by the Coast and Cascade Mountain Ranges,

the plateau exists in a rain shadow, resulting in limited annual precipitation of only 300-400 mm (Tutolo et al. 2024). This region's semi-arid climate, paired with high summer evaporation rates, intensifies its unique hydrological characteristics and creates favorable conditions for high-solute environments (Renaut and Long 1989; Nesbitt 1990; Tutolo and Tosca 2023).

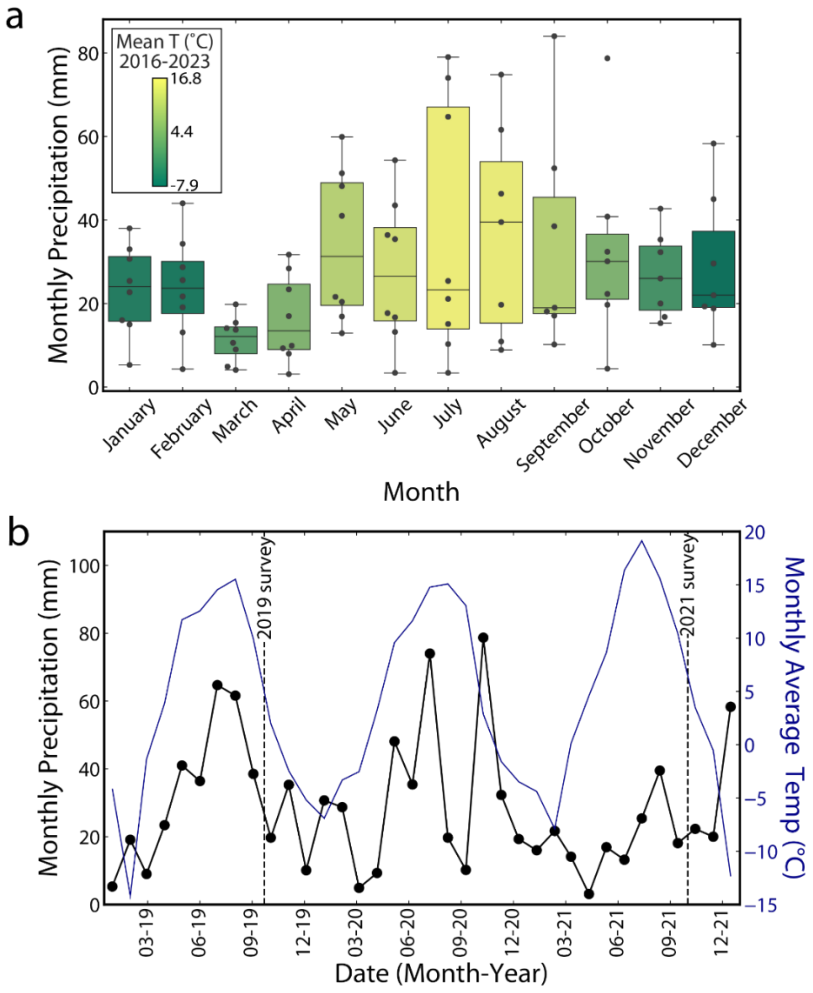

Figure 3: (a) Monthly precipitation recorded at the Clinton RCS weather station, with boxes colored to represent mean monthly temperature. (b) Monthly precipitation and average temperature from January 2020 to December 2021. Figure from Tutolo et al. (2024).

Geologically, the Cariboo Plateau was shaped by significant volcanic activity during the Miocene epoch, producing extensive basalt flows of the Chilcotin Group that now form its bedrock (Mathews 1989; Tribe 2005). These flat-lying basaltic formations overlie older Mesozoic

sedimentary rocks, which are interlaid with glacial and fluvial deposits from Pleistocene glaciations, creating a multi-layered geological structure (Campbell and Tipper 1971; Russell et al. 2023). Repeated glacial advances and retreats shaped the plateau's rolling hills, drumlins, and closed depressions, which trap seasonal meltwater and support the formation of alkaline lake systems (Dohaney 2006). The hydrological isolation of these basins limits outflow, while interactions with the basaltic bedrock provide a steady influx of ions like calcium, magnesium, and silica (Gislason and Oelkers 2003). These processes create conditions conducive to high pH and stable dissolved carbonate concentrations, further promoting the precipitation of evaporite minerals such as dolomite (Siegel 1961; Renaut and Long 1989).

Last Chance Lake, located on the Cariboo Plateau, is the world's most phosphate-rich lake, with concentrations reaching up to 37 mM (Toner and Catling 2020). This makes it a central focus in addressing the "phosphate problem" in prebiotic chemistry, as its high phosphate levels support hypotheses about the accumulation of biomolecule precursors on early Earth (Toner and Catling 2020). Unlike many lakes, where dissolved phosphate is rapidly removed through the precipitation of insoluble calcium-phosphate minerals like apatite, Last Chance Lake's elevated carbonate content sequesters calcium as low-solubility Ca^{2+} carbonates (Toner and Catling 2020).

Seasonal evaporation cycles further enhance the lake's salinity and alkalinity, concentrating dissolved ions throughout the warmer months (Renaut and Long 1989; Renaut 1990). Visually, the lake is opaque and cloudy, particularly during late summer, as mineral concentrations peak and is marked by a network of desiccation patterns (Fig. 4). Despite its extreme phosphorus concentrations, Last Chance Lake lacks dense microbial mats, likely due to its limited nitrogen availability and high salinity (Zorz et al. 2019; Haas et al. 2024). This dampened biological activity makes it an ideal natural laboratory for differentiating between biological and geochemical influences on phosphorus cycling (Schultze-Lam et al. 1996; Haas et al. 2024).

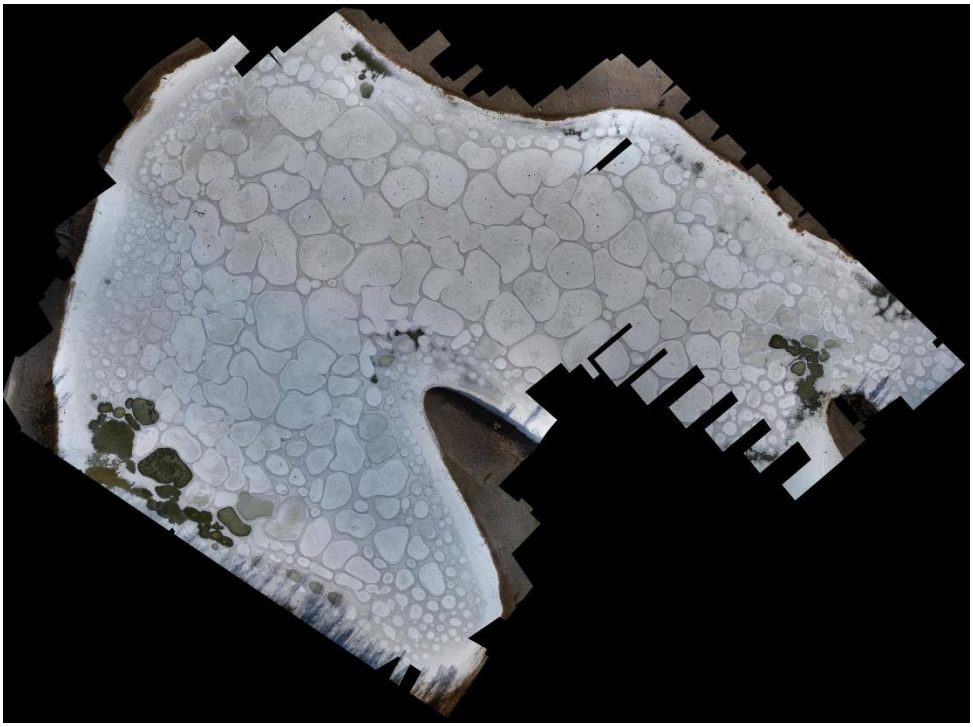

Figure 4: Drone image of Last Chance Lake, October 2022, taken by Dr. Tutolo, showing rounded salt crust patterns across the nearly dry lake surface.

Goodenough Lake, in contrast, is a biologically prolific system dominated by extensive microbial mats composed primarily of cyanobacteria (Schultze-Lam et al. 1996). These mats, which range in color from light to dark green, create visible textures and layering across the lakebed (Zorz et al. 2019). The lake's pH consistently hovers around 10.2, creating a stable alkaline environment that supports robust and dynamic microbial communities. Groundwater input provides consistent recharge, maintaining the lake's hydrological balance (Tutolo et al. 2024) and supporting its biogeochemical activity.

Figure 5: Photograph of Goodenough Lake in October 2022, showing moderate water levels with visible salt crust deposits along the shoreline.

The microbial mats in Goodenough Lake play a significant role in nutrient cycling, actively processing nutrients such as phosphorus. During the summer, biological activity intensifies, expanding the mats and increasing phosphorus uptake from the water (Zorz et al. 2019; Haas et al. 2024). This biologically driven nutrient retention contrasts sharply with the largely abiotic processes observed in Last Chance Lake, offering a comparative framework for studying phosphorus cycling in high-pH environments.

In sum, the differences between Last Chance and Goodenough Lakes show the diversity of geochemical and biological processes within alkaline lake systems. Last Chance Lake's high-phosphate, low-biological-activity environment provides a model for studying abiotic nutrient dynamics, while Goodenough Lake's active microbial mats demonstrate the impact of life on nutrient cycling and retention. Together, these lakes illustrate how varying degrees of biological activity influence nutrient availability and mineral formation, offering critical insights into the environments that may have supported the origins of life on Earth.

1.4.2 The Basque Lakes Environment

The Basque Lakes, located in the Thompson Plateau as described by Renaut and Stead (1994) and shown in Figure 2, are a series of closed-basin, magnesium-sulfate ($MgSO_4$)-saturated playas that exemplify extreme geochemical conditions and brine evolution (Renaut and Stead 1994). These

saline lakes provide contrast to the alkaline lakes of the Cariboo Plateau, serving as natural laboratories for understanding how hydrological and geochemical processes drive the formation of dense brines, as they typically exhibit pH levels around 7-8.5, reflecting different chemical dynamics. Their mineralogies make them critical analogues for extraterrestrial environments, particularly for studying biosignature preservation in hypersaline conditions. To illustrate the nature of each Basque Lake, photos are provided below in Figures 6-9.

Figure 6: Panoramic view of Basque Lake 1, October 2022.

Figure 7: Basque Lake 2, October 2022, showing distinct individual pools within the larger basin, divided by mineral crusts.

Figure 8: Basque Lake 3, April 2023, showing a distinct reddish coloration caused by the presence of brine shrimp, with salt crust deposits visible along the shoreline.

Figure 9: Basque Lake 4, October 2022, showing minimal water remaining after the summer, with the lakebed covered in salt deposits.

The Thompson Plateau, part of British Columbia's Interior Plateau, is geologically diverse, shaped by volcanic activity, tectonic processes, and extensive glacial history. The Basque Lakes basin is underlain by the greenstones, argillites, and cherts of the Cache Creek Terrane, which significantly influence the chemical composition of these lakes (Renaut and Stead 1994). Also beneath the Basque Lakes is an ash deposit, which acts as an aquifer (Nesbitt 1990), from the Mount Mazama eruption approximately 7,640 years ago (Zdanowicz et al. 1999). Overlying these ancient terranes are glacial and fluvial deposits that form the clay-rich natural dams separating the individual lakes (Goudge 1926). These geological barriers limit water flow between the lakes, reinforcing their closed-basin nature.

The physical landscape surrounding the Basque Lakes is characterized by saline mud flats, sparse vegetation, and esker hills formed during glacial retreat. These features, combined with the region's low annual precipitation (~300-400 mm) and high summer evaporation rates, contribute to intense solute accumulation within the lake basins (Renaut and Long 1989; Nesbitt 1990). Seasonal inputs from snowmelt in spring create a temporary reduction in salinity, but this is quickly reversed during

the summer months as evaporation surpasses precipitation, leading to the steady formation of dense brines (Crisler et al. 2019).

The hydrology of the Basque Lakes is defined by seasonal variability, with limited recharge and restricted drainage enhancing solute retention. During spring, snowmelt and rainfall temporarily dilute the lake water, lowering solute concentrations. However, intense summer evaporation drives the formation of highly concentrated Mg-SO_4-Cl brines, creating one of North America's most magnesium-rich systems (Renaut and Long 1989; Nichols et al. 2023). The resulting geochemistry supports the precipitation of hydrous magnesium, sodium, and calcium salts.

Minerals precipitated in the Basque Lakes include gypsum ($CaSO_4 \cdot 2H_2O$), magnesite ($MgCO_3$), epsomite ($MgSO_4 \cdot 7H_2O$), bloedite ($Na_2Mg(SO_4)_2 \cdot 4H_2O$), and mirabilite ($Na_2SO_4 \cdot 10H_2O$) (Raudsepp et al. 2024). These minerals are particularly abundant in Basque Lakes 1 and 2, where the largest deposits are found (Goudge 1926). The economic importance of these deposits is evidenced by historical mining operations in Basque Lake 1, where sodium and magnesium salts were extracted for commercial use (Cummings 1940).

The Basque Lakes provide a terrestrial analogue for brine-rich extraterrestrial systems, where similar geochemical conditions might support microbial life. Specifically, they are of significant interest to astrobiologists due to their high concentrations of $MgSO_4$ brines, which resemble those hypothesized to have existed on ancient Mars (Gendrin et al. 2005; Chipera et al. 2023) and detected on icy moons such as Europa and Enceladus (Fox-Powell and Cockell 2018; Buffo et al. 2022). Therefore, research of these systems may enhance the collective understanding of how high-salinity environments might sustain microbial life or preserve biological signals over time.

1.5 Stable Oxygen Isotope Ratios and Fractionation

Stable oxygen isotopes (^{16}O and ^{18}O) serve as powerful tools for deciphering environmental processes, offering insights into hydrology, geochemistry, and biological cycling (Urey 1947; Craig 1961). During evaporation, water molecules containing the lighter ^{16}O isotope preferentially enter the vapor phase, while molecules with the heavier ^{18}O tend to remain in the liquid phase (Lloyd 1964). This selective fractionation occurs because lighter molecules have higher kinetic energy at a given temperature, making them more likely to overcome the liquid's surface tension

and evaporate. Epstein's work (Epstein et al. 1953) demonstrated how these isotopic signatures could be preserved in carbonate minerals, while Talbot (1990) showed how they record changes in hydrological conditions, particularly in systems dominated by evaporation (Talbot 1990).

This systematic discrimination during evaporation and subsequent condensation processes and rainout effects creates predictable patterns in the isotopic composition of global precipitation, driven by the slight mass differences between isotopes of water. The relationship between oxygen and hydrogen isotopes in precipitation follows a consistent trend known as the Global Meteoric Water Line (Craig 1961). This relationship emerges from the coupled behavior of oxygen and hydrogen isotopes during evaporation and condensation cycles, providing a framework for understanding global water circulation patterns and identifying waters that have undergone evaporation or other processes that deviate from typical meteoric conditions.

These early contributions not only established the theory of isotope geochemistry but also demonstrated its practical applications. The measurement of isotopic ratios, expressed in delta (δ) notation, enables tracking of isotopic variations and is defined below as modified from McKinney et al., (1950):

$$\delta = \left(\frac{R_x - R_{std}}{R_{std}}\right) \times 1000 \text{ (Sharp 2017)} \quad (3)$$

where R represents the ratio of heavy to light isotopes (e.g., $^{18}O/^{16}O$), x denotes the sample, and std is the standard, the ratio is multiplied by 1000 for clarity. δ-values are reported in per mil (‰). A positive δ-value indicates enrichment in the heavier isotope relative to the standard, while a negative δ-value signifies depletion (Sharp 2017). For example, $^{18}O/^{16}O$ can be characterized as $\delta^{18}O$ and is usually referenced to Vienna Standard Mean Ocean Water (VSMOW). This standardized approach reliably traces environmental processes. Stable isotope ratios of a given element can be measured exclusively within a specific compound. Of particular importance for this thesis is the measurement $\delta^{18}O$ within PO_4^{3-}, which is commonly expressed as $\delta^{18}O_{PO_4}$.

1.5.1 Oxygen Isotope Fractionation in Water ($\delta^{18}O_{H_2O}$)

Oxygen isotope ratios in water ($\delta^{18}O_{H_2O}$) are highly useful for understanding hydrological processes, particularly in closed-basin lakes where evaporation plays a dominant role in shaping isotopic signatures. Fractionation occurs during phase changes, such as evaporation, as lighter isotopes (^{16}O) are preferentially removed into the vapor phase due to their lower energy requirements. The residual water becomes progressively enriched in the heavier isotope (^{18}O), resulting in higher $\delta^{18}O_{H_2O}$ values (Urey 1948; Epstein et al. 1953; Gat 1981; Kendall and McDonnell 1998). This enrichment process is particularly pronounced in arid or semi-arid environments, where evaporation often exceeds precipitation, and outflow is minimal.

In systems like the lakes studied here, seasonal variations in evaporation and precipitation significantly influence $\delta^{18}O_{H_2O}$ values. During the dry summer months, evaporation intensifies, leaving the remaining water enriched in ^{18}O. This isotopic enrichment reflects the difference in saturated vapor pressures between isotopologues, with ^{16}O-bearing water molecules preferentially entering the vapor phase (Xinping et al. 2005). Conversely, during the wetter spring months, snowmelt and precipitation introduce isotopically lighter water, decreasing the $\delta^{18}O_{H_2O}$ values.

The closed-basin nature of the Interior Plateau lakes amplifies the effects of evaporation on $\delta^{18}O_{H_2O}$. Unlike open systems with significant outflow, these lakes retain water until it is removed almost exclusively through evaporation. Thus $\delta^{18}O_{H_2O}$ can serve as a sensitive recorder of water balance and climatic variability. The absence of outflow also means that changes in $\delta^{18}O_{H_2O}$ reflect not only seasonal dynamics but also longer-term hydrological trends, making these lakes ideal natural laboratories for studying evaporative processes in semi-arid environments (Lloyd 1964; Talbot 1990). To further compare the isotopic evolution of waters within these lakes, the GMWL (Global Meteoric Water Line), defined by Craig (1961), which follows the relationship $\delta^{2}H_{H_2O} = 8\ \delta^{18}O_{H_2O} + 10$, and the OMWL (Okanagan Meteoric Water Line), derived for the region by Wassenaar et al. (2011), which follows a slope of $\delta^{2}H_{H_2O} = 6.6\ \delta^{18}O_{H_2O} - 22.7$, will serve as useful comparisons to track these hydrological systems (Wassenaar et al. 2011).

The relationship between ambient water and intracellular water within organisms is an important consideration. Intracellular water typically approaches isotopic equilibrium with the surrounding environmental water due to isotopic exchange processes, particularly in aquatic systems where

organisms continuously interact with ambient water as the system pushes towards a homogenous state (Fry 2006).

1.6 Oxygen Isotopes in Phosphate ($\delta^{18}O_{PO_4}$)

The analysis of oxygen isotopes in phosphate ($\delta^{18}O_{PO_4}$) is a valuable tool for tracing phosphorus cycling across terrestrial and aquatic ecosystems. This method derives its power from the stability of the phosphorus-oxygen (P-O) bond, which remains intact under typical environmental conditions, preserving the isotopic signature through both biotic and abiotic processes (Winter et al. 1940). The stability of this bond allows $\delta^{18}O_{PO_4}$ to serve as a reliable indicator of phosphorus transformations in natural systems, even in the absence of biological activity (Blake et al. 1997; McLaughlin et al. 2006; Pfahler et al. 2022).

Phosphorus, primarily existing as phosphate (PO_4^{3-}), binds to oxygen and participates in dynamic cycling driven by geochemical and biological processes. Geochemical processes, such as precipitation, dissolution, adsorption, and desorption, play critical roles in phosphorus turnover. Biological processes, including remineralization and intracellular cycling, further enhance its dynamic nature (Arai and Sparks 2007; Kauwenbergh 2010; Vos et al. 2014). The ability of $\delta^{18}O_{PO_4}$ to reflect these transformations allows researchers to distinguish between abiotic processes, such as mineral dissolution, and biological processing, such as enzymatic cleavage (Blake et al. 1997).

Isotope fractionation, which describes the preferential partitioning of isotopes during physical, chemical, or biological processes, is the basis of using $\delta^{18}O_{PO_4}$ as a tracer. Fractionation occurs because isotopes differ slightly in mass, and this difference affects bond strength and reaction behavior (Dauphas and Schauble 2016). Heavier isotopes, such as ^{18}O, form stronger chemical bonds than lighter isotopes, such as ^{16}O, leading to distinct fractionation patterns. These patterns are governed by two primary mechanisms: kinetic fractionation and equilibrium fractionation (Hoefs 2009; Davies et al. 2014).

Kinetic fractionation arises in unidirectional reactions, where lighter isotopes, like ^{16}O, react more quickly and diffuse more easily due to their lower energy requirements. As a result, the reaction product becomes enriched in the lighter isotope, leading to negative isotopic shifts in its $\delta-$value.

In the context of $\delta^{18}O_{PO_4}$, biological processes such as enzymatic activity frequently exhibit kinetic effects (Liang and Blake 2006a). For instance, enzymes such as acid and alkaline phosphatases cleave phosphate bonds, preferentially incorporating ^{16}O into reaction products. These processes typically result in fractionation factors ranging from -10 ‰ to -25 ‰ (Liang and Blake 2006b; Shen et al. 2020).

In contrast, equilibrium fractionation occurs during reversible reactions, where oxygen isotopes continuously exchange between reactants and products until a stable distribution is achieved. Heavier isotopes, like ^{18}O, tend to stabilize in lower-energy states, resulting in their preferential incorporation into substances with stronger bonds, such as liquid water or solid phases (Hoefs 2009; Davies et al. 2014). Equilibrium fractionation is strongly temperature-dependent, with larger fractionation effects occurring at lower temperatures (Epstein et al. 1953; Chang et al. 2021).

The distinction between kinetic and equilibrium fractionation can be nuanced. This is exemplified by the enzyme inorganic pyrophosphatase (PPase), which catalyzes the complete exchange of all four oxygen atoms in pyrophosphate ($P_2O_7^{4-}$) with intracellular water.

$$P_2O_7^{4-} + H_2O \rightarrow 2(PO_4^{3-}) \quad (5)$$

In Eq. (5) PPase is catalyzing a kinetic, unidirectional reaction. However, because intracellular water is typically in equilibrium with the surrounding water, and all four oxygen atoms are exchanged, the $\delta^{18}O_{PO_4}$ of phosphate that has been processed via PPase reflects that of the $\delta^{18}O_{H_2O}$ of the equilibrated environment (Chang et al. 2021). In sum, the phosphate oxygen undergoes a kinetic process that is ultimately masked by the prevailing equilibrium conditions.

Abiotic processes also influence $\delta^{18}O_{PO_4}$ values, though typically to a lesser extent than biological mechanisms. For example, the precipitation and dissolution of phosphate minerals, such as apatite, can subtly alter the oxygen isotopic composition of dissolved phosphate. Additionally, adsorption onto mineral surfaces, particularly iron oxides, can lead to positive shifts in $\delta^{18}O_{PO_4}$ values (Jaisi et al. 2010; Adu-Gyamfi and Pfahler 2022). Variations in temperature and the isotopic composition of surrounding water ($\delta^{18}O_{H_2O}$) further complicate these abiotic fractionation pathways, making careful interpretation of $\delta^{18}O_{PO_4}$ values critical (Melby et al. 2013).

Overall, the relationship between $\delta^{18}O_{PO_4}$ and $\delta^{18}O_{H_2O}$ is particularly significant in both biological and abiotic systems. In biological systems, $\delta^{18}O_{PO_4}$ can reflect the isotopic composition of intracellular water (and, by extension, environmental water), specifically in processes mediated by PPase. In abiotic systems, $\delta^{18}O_{PO_4}$ is directly influenced by the $\delta^{18}O_{H_2O}$ of environmental water, particularly during equilibrium-driven reactions like precipitation and dissolution (Blake et al. 1997; Tamburini et al. 2014). This isotopic linkage allows researchers to connect phosphate-water interactions to environmental conditions, such as temperature, water composition, and biological activity (Larsen et al. 1989; Jaisi and Blake 2014; Lis et al. 2019).

1.7 Goals of this Study

1.7.1 Research Aim

This study aims to evaluate the geochemical behavior of phosphorus in saline lake environments and evaluate the relevance of this behavior for the origin of life on planetary surfaces. To do this, we evaluate biological utilization of phosphate through analysis of the oxygen isotopic composition of dissolved phosphate ($\delta^{18}O_{PO_4}$) and coexisting lake waters ($\delta^{18}O_{H_2O}$) over two summer seasons and compare against expected values. This approach allows for an assessment of phosphate utilization within these lake systems, distinguishing between biological and chemical cycling processes.

Historically, phosphate isotopic analyses have been performed on more dilute and/or less alkaline waters. Thus, successful execution of the research within this thesis required methodological development. The primary objective is to quantitatively precipitate dissolved phosphate in the form of a pure silver phosphate analyte. Care must be taken to minimize residual silver, in turn avoiding the formation of silver oxide coating under UV exposure. As such, the employed methodology builds on the silver phosphate precipitation protocol established by Tamburini et al. (2010), with specific modifications to accommodate the high salinity and alkalinity of these lake samples. Ultimately, this refined methodology (see **Section 2.5**) represents a significant outcome of the presented research in addition to the main science outcomes because it establishes a reliable approach for $\delta^{18}O_{PO_4}$ analysis in hypersaline, alkaline, and analogous environments.

1.7.2 Hypothesis

To direct the presented research, I offer the following hypothesis:

Given the apparent, inorganic controls on its phosphorus concentrations I hypothesize that Last Chance Lake and the hypersaline, phosphate-limited Basque Lakes will show less biological control of its phosphate isotopic signatures compared to neighboring, more biologically active Goodenough Lake.

Testing this hypothesis in the context of origins-of-life chemistry will permit better understanding of the relevance for these saline lake environments for hosting the construction of the first building blocks of life on Earth and/or Mars.

2. Methods

2.1 Sampling and Procedure

Sampling was conducted in October 2022 and 2023, as well as in April 2023 and 2024, across the Last Chance, Goodenough, and Basque Lakes (BL1-BL4). Generally, samples were acquired at a water depth of 20-50 cm via 1 L Low-Density Polyethylene (LDPE) bottles, but, in instances where lake levels were too low to permit sampling in this manner, syringes were used. Where possible, samples were collected a few meters' distance from the shoreline to ensure representative chemistry. Initial filtration was performed using Millipore Millex-HV 0.45 μm hydrophilic PVDF syringe filters in the field. This process was labour-intensive due to high particulate content, which strained the filters. In some instances, peristaltic pumps were employed to expedite filtration, though hand-filtering via syringe was necessary for certain samples. Field measurements, including pH, temperature, and electrical conductivity (EC) were recorded using a Thermo Scientific Orion Star A329 portable multimeter, calibrated via NIST-traceable buffers at least once daily. Alkalinity was assessed as soon as possible after sampling (generally later the same day) with a Thermo Scientific Orion Star T910 pH Titrator using 0.02 N H_2SO_4 acid by diluting 0.1 ml of sample with 0.9 ml deionized water. After collection, samples were stored in sealed bottles until subsequent analyses could be performed, with cation samples acidified in the field using 10 % trace metal grade HCl.

Upon return to Calgary, samples were further filtered using 0.2 μm PVDF filters to ensure removal of fine particulates prior to the silver phosphate precipitation procedure. For each lake, sampling was carefully adapted to site-specific conditions. At Last Chance and Goodenough Lakes, samples were collected several meters from the shore to avoid isolated evaporative pools, with precautions taken to minimize the disturbance of silt and mud. In BL2, water was drawn from the same evaporative pools used for lake sediment coring (in the context of a separate study); typically, larger and deeper pools with muddy bottoms were deemed suitable for coring activities. Sampling at BL1 was only possible when sufficient water remained, generally from the largest pool, as this lake is often dry by October.

BL3 provided relatively straightforward sampling due to a sturdy salt crust covering the lakebed (Fig. 8), allowing for sample collection at the lake's deepest accessible point, which was typically less than 1 meter above the salt layer. BL4, however, posed more challenges, particularly in October when extensive evaporation left only shallow water. For these samples, water was drawn via syringe from the surface layer to avoid disturbing the muddy bottom. In April, sampling in BL4 was conducted near the water surface, as stirring up sediment was unavoidable in the lake's softer, muddier areas. BL4 also is prone to complete desiccation and water present in October 2022 was limited (Fig. 9). Each lake sample was handled independently without pooling to ensure accurate representation of individual lake conditions.

2.2 Cation and Anion Analysis

Upon return to Calgary, samples were diluted and measured using Ion Chromatography (IC) for anions, while hydrochloric acid dilution was used for cation measurement using Inductively Coupled Plasma-Optical Emission Spectroscopy (ICP-OES). Dilution was accounted for during the processing of each sample. Phosphorus concentrations were measured primarily through a spectrophotometric method using an automated Thermo Scientific™ Gallery™ system, with a precision of ±5 %. This analytical technique involves a series of chemical reactions designed to accurately quantify orthophosphate ions in the sample. Initially, orthophosphate ions react with ammonium molybdate and an antimony potassium tartrate catalyst under acidic conditions, leading to the formation of a 12-molybdophosphoric acid complex. This intermediate complex is then reduced using ascorbic acid, resulting in the development of a blue-colored compound. The

intensity of this color is directly proportional to the orthophosphate concentration and is measured spectrophotometrically. To determine the concentration of orthophosphate in the sample, the measured absorbance is compared to a calibration curve, which is constructed from standards of known concentrations.

2.3 Water Isotope Analysis

Isotopic analysis of the stable water isotopes $\delta^2H_{H_2O}$ and $\delta^{18}O_{H_2O}$ were performed at the Stable Isotope Lab at the University of Calgary using a Thermo Finnigan Delta V continuous Flow-Isotope Ratio Mass Spectrometry (CF-IRMS) with a Thermo GasBench instrument attached. All results were reported in the usual permil notation relative to IAEA: VSMOW-SLAP-GISP with respective values (‰) of 0, -55.5, and -24.8 for $\delta^{18}O_{H_2O}$ and 0, -428, and -189.5 for $\delta^2H_{H_2O}$. The reported precision and accuracy, as 1 sigma of (n=10) lab standards were 0.25 ‰ for $\delta^{18}O_{H_2O}$ and 4.0 ‰ for $\delta^2H_{H_2O}$.

2.4 Oxygen Isotope Analysis of Dissolved Phosphate

To analyze oxygen isotopes in dissolved PO_4^{3-}, a detailed multi-step procedure was employed, primarily based on the protocol established by Tamburini et al. (2010). The initial steps involved concentrating dissolved phosphate through co-precipitation, followed by several additional purification stages to achieve the desired analyte purity, as described below.

2.4.1 Magnesium-Induced Co-precipitation (MagIC)

The first purification step, adapted from Karl and Tien (1992), was Magnesium-Induced Co-precipitation (MagIC), which aimed to concentrate dissolved phosphate and reduce the sample volume needed for adequate Ag_3PO_4 precipitation (Karl and Tien 1992). Initially, samples were treated with a 1 M sodium hydroxide solution, which was added gradually until the sample reached a pH of approximately 9.5. In Basque Lake samples, this procedure successfully produced a brucite precipitate, which allowed for effective phosphate concentration. Once brucite precipitation was achieved, the floc was collected by centrifugation and subsequently redissolved in approximately 5 mL each of concentrated acetic acid and 10 N nitric acid. Deionized water was then added to

adjust the final sample volume to around 200 mL. However, in Last Chance and Goodenough Lake samples, brucite precipitation did not occur, apparently due to aspects of the lake chemistry (i.e., the highly elevated alkalinity of both lakes).

2.4.2 Cation Exchange Resin

The second step involved passing the samples through a cation exchange resin column, which had been conditioned with 7 N nitric acid and thoroughly rinsed with deionized water before sample addition. The samples were passed through the column by gravity, without added pressure, to avoid disturbing the exchange process; however, slight manual pressure was applied with syringes if flow issues occurred. This step resulted in the removal of most of the cations present in the samples, significantly reducing their concentrations, but not completely eliminating them. After passing through the column, the samples were collected in 250 mL bottles and held for the next purification step.

2.4.3 Ammonia Phosphomolybdate (APM) Precipitation

To precipitate the phosphate as ammonia phosphomolybdate (APM), I followed a procedure adapted from Tamburini et al. (2010). The samples were transferred to Erlenmeyer flasks and placed on a stir plate in a 50°C water bath, with a magnetic stirrer to ensure uniform mixing. A solution containing 25 mL of 35 % ammonium nitrate and 40 mL of 10 % NH_4-Mo was added to each sample. Due to the high alkalinity of the samples, the addition of 0.5-1.0 mL H_2SO_4 recommended by Tamburini et al. (2010) was insufficient to lower the pH to the target range of 1-2. Therefore, additional H_2SO_4 was added to reach the necessary pH, allowing the color change from green to yellow and facilitating APM precipitation. The samples were then covered and left to stir gently overnight. If no APM deposits were observed the following morning, the pH was rechecked and adjusted if necessary, and samples were left to stir for an additional night. The APM crystals were collected via vacuum filtration using 0.2 µm PVDF filters, while the excess solution was discarded. The crystals and flasks were rinsed three to four times with 5 % ammonium nitrate to ensure thorough collection of the APM crystals. The collected crystals were dissolved in a small amount of citric acid in preparation for subsequent processing.

2.4.4 Magnesium Ammonia Phosphate (MAP) Precipitation

For the MAP precipitation, new flasks were placed on stir plates, and 25 mL of magnesia solution (50 g $MgCl_2$ and 100 g NH_4Cl dissolved in 500 mL of deionized water, acidified to pH 1 with concentrated HCl) was added to each sample. The pH was then raised to above 9 by slowly adding approximately 7 mL of a 1:1 NH_4OH water solution. After stirring overnight, the MAP crystals were collected through the same filtration method used for APM crystals. These crystals were rinsed with a 1:20 NH_4OH water solution to remove excess chloride. The crystals were then redissolved in 17.5 mL of 0.5 N HNO_3 within 50 mL tubes.

2.4.5 Second Cation Exchange Resin Treatment

After redissolution of the MAP crystals, the solution was passed through a cation exchange resin conditioned with 7 N HNO_3 and thoroughly rinsed. This step was repeated to ensure the removal of residual cations, leaving a purified solution of dissolved phosphate for the final silver phosphate precipitation step.

2.4.6 Silver Phosphate Precipitation

The final step, silver phosphate precipitation, was adapted to account for the highly alkaline and saline nature of the samples, which hindered effective chloride removal in earlier steps. For samples that successfully underwent brucite precipitation via the MagIC method, this additional chloride removal step was not required. The key reagents for this stage were a 2:1 NH_4OH water solution, 7.8 N HNO_3, and pure silver nitrate crystals.

The sample was placed in a disposable cup with a pH probe and stirrer, and the initial pH was adjusted to ~7.5 by slowly adding the 2:1 ammonia solution. Small increments of pure silver nitrate (~0.005 g) were added, and if a white AgCl precipitate formed immediately, it was filtered out. The supernatant was collected, and the process repeated until minimal AgCl formed. To avoid inadvertently filtering out Ag_3PO_4, if silver chloride crystals appeared, the pH was dropped to ~1 using 7.8 N HNO_3, which redissolved the Ag_3PO_4 but left silver chloride as a solid for easier removal. After filtering out AgCl, the pH was raised back to ~7.5. Once no further AgCl was

observed, an excess of silver nitrate was added, resulting in the formation of yellow, pure Ag_3PO_4 crystals.

The reaction described as:

$$PO_4^{3-} + 3\ AgNO_3 \rightarrow Ag_3PO_4 + 3\ NO_3^- \quad (6)$$

required constant pH monitoring due to the buffering action of phosphate ions. If the pH dropped during the addition of silver nitrate, more 2:1 ammonia solution was added to maintain pH ~7.5, as Ag_3PO_4 will dissolve in lower pH conditions. Filtration was performed promptly using a compact 13.5 mm diameter filtration apparatus and 0.22 µm PVDF filters to prevent the Ag_3PO_4 from dispersing or passing through the filter, as the crystals tend to adhere strongly to a large filter surface area. After filtration, the crystals were rinsed with deionized water to remove excess silver ions, which, if left, would form a silver oxide coating under UV exposure. While this coating did not have a significant effect on isotopic measurements, as presented in Table 3, it is advisable to remove it where possible.

Finally, the samples were stored on the filters in glass vials, shielded from light, until they were weighed into tin capsules for $\delta^{18}O_{PO_4}$ analysis. This iterative pH adjustment and selective precipitation method was necessary to counteract the high chloride levels in the samples. For samples that did not undergo MagIC step brucite precipitation, this final step effectively separated AgCl, preserving phosphate in solution. As a final quality check, excess silver nitrate was added to the supernatant post-filtration, and if additional Ag_3PO_4 precipitated, it was filtered and combined with the main sample to prevent fractionation effects. Quality of the final analyte was verified using SEM (Scanning Electron Microscopy) to ensure ratios of Ag:O:P were 3:4:1. Most samples underwent a single precipitation stage, with any isotopic variations checked during $\delta^{18}O_{PO_4}$ analysis to account for the effects of silver oxide formation on the isotopic ratios. For samples that underwent multiple precipitation stages, it is recommended that homogenization of the precipitated Ag_3PO_4 occurs before sample analysis due to a fractionating effect as presented in Table 3.

2.4.7 Oxygen Isotope Analysis of Ag_3PO_4

Analysis was conducted at The Stable Isotope Laboratory at the University of Lausanne (UNIL). The Ag_3PO_4 was thermally decomposed to release oxygen gas, which was subsequently converted to carbon dioxide for isotopic analysis. Using a Finnigan MAT 253 high-precision isotope-ratio mass spectrometer (IRMS), the oxygen isotope ratios were measured along with USGS-80 and 81 reference materials, and results were reported relative to the VSMOW scale. The reference materials both displayed a standard deviation of 0.3 ‰ or better across two sample runs (n = 9 for both reference materials in each run).

2.5 Calculation of Equilibrium

Oxygen isotopes within phosphate ($\delta^{18}O_{PO_4}$) are influenced by biological processes, especially enzymatic reactions that drive isotopic exchange between phosphate and water (see **Section 1.6**). To calculate the equilibrium $\delta^{18}O_{PO_4}$ values in this study, I use the equation developed by Chang and Blake (2015), which accounts for the conditions under which oxygen is exchanged between water and phosphate via PPase (Chang and Blake 2015):

$$\delta^{18}O_{PO_4EQ} = -0.18T + 26.3 + \delta^{18}O_{H_2O} \quad (7)$$

Where $\delta^{18}O_{PO_4EQ}$ represents the equilibrium $\delta^{18}O_{PO_4}$ of phosphate in water and is hereon referred to as the expected equilibrium value. T is temperature in °C and $\delta^{18}O_{H_2O}$ is the $\delta^{18}O$ value of the surrounding water.

To quantify the degree of disequilibrium between measured (Table 2) and expected values, I calculate and define the capital delta ($\Delta\delta^{18}O_{PO_4}$) value as:

$$\Delta\delta^{18}O_{PO_4} = \delta^{18}O_{PO_4EQ} - \delta^{18}O_{PO_4\,Measured} \quad (8)$$

where $\delta^{18}O_{PO_4EQ}$ is the expected equilibrium value calculated using Equation 7, and $\delta^{18}O_{PO_4\,Measured}$ is the actual measured value. A positive $\Delta\delta^{18}O_{PO_4}$ value indicates the measured value is lower than equilibrium predictions, while a negative value suggests the measured value exceeds equilibrium predictions.

Chang and Blake (2015) derived this equation through precise calibration of equilibrium oxygen isotope fractionations between dissolved phosphate and water over a temperature range of 3 to 37 °C. Their methodology involved controlled laboratory experiments combined with modern CF-IRMS TC/EA analysis of Ag_3PO_4. It is specific to equilibrium fractionation between dissolved phosphate and water and is thus appropriate for use in oxygen isotope studies of dissolved phosphate using the method outlined above.

Table 1: General Fluid Chemistry

Sample ID	PO4 (mmol/L)	Cl (mmol/L)	Na (mmol/L)	Ca (mmol/L)	Mg (mmol/L)	K (mmol/L)	SO4 (mmol/L)	Alkalinity (eq/L)	pH	EC (mS/cm)
BL3 Oct, 22	0.03	78.98	940.08	8.13	1563.52	41.77	1989.27	0.09	7.74	61.22
BL4 Oct, 22	0.19	13.68	716.82	7.28	1421.36	18.13	1818.47	0.01	7.51	64.37
GE Oct, 22	0.05	70.11	923.19	0.1	3.4	16.02	19.87	0.8	10.27	55.51
GE Apr, 23	0.05	21.63	262.85	0.04	1.13	5	6.13	0.23	10.36	25.65
LC Apr, 23	0.57	27	552	0.06	0.34	3.67	29.78	0.47	10.21	45.31
LC Apr, 23	0.54	26.12	533.69	0.29	0.48	3.53	28.8	0.49	10.32	47.33
BL1 Oct, 23	0.17	64.57	510.31	7.38	937.43	43.53	2008.86	0.02	7.86	55.16
LC Oct, 23	11.82	161.78	1441.39	0.03	1.76	71.17	84.25	1.18	9.16	104.8
LC Dec, 23	1.7	161.78	895.59	0.13	0.65	8.01	90.37	0.86	9.16	104.8
BL1 Apr, 24	0.14	27.52	606.24	14.57	1021.42	23.1	1817.46	0.02	7.8	56.19
BL2 Apr, 24	0.02	26.25	503.02	18.51	877.39	18.81	1224.25	0.05	8.25	66.36
BL3 Apr, 24	0.03	92.45	960.58	11.54	1316.35	46.99	2262.78	0.1	7.88	56.02
BL4 Apr, 24	0.001	19.57	602.59	20.34	668.8	17.9	1118.35	0.01	9.26	66.42
GE Apr, 24	0.05	51.91	625.27	0.07	2.08	11.8	17.26	0.13	10.4	41.98
LC Apr, 24	1.59	88.17	1307.84	0.07	0.41	9.77	97.03	0.4	10.16	74.1

3. Results

3.1 Fluid Chemistry

Analyses of the chemical composition of lake waters from Basque Lakes, Goodenough Lake, and Last Chance Lake reveal distinct variations in solute concentrations among the systems (Table 1).

These results were compared to previously published data from studies on these lakes (Toner and Catling 2020; Haas et al. 2024). The findings are categorized and summarized below.

3.1.1 Phosphate Concentrations Across Lake Systems

Phosphate concentrations varied significantly across the six lakes, with Last Chance Lake (LC) exhibiting the highest values among all systems. In October, LC reached a peak phosphate concentration of 12 mmol/L, compared to its April value of 0.5 mmol/L, reflecting an order-of-magnitude increase during the summer evaporation cycle, a result consistent with previous studies labelling LC as having one of the highest dissolved phosphate concentrations on Earth (Hirst 1995; Toner and Catling 2020). A related sample, LC Dec, 23, represents the same water collected in October 2023 but left unfiltered for two months. The phosphate concentration in this sample measured 1.7 mmol/L, significantly lower than the filtered LC Oct, 23 sample. Goodenough Lake (GE), by contrast, displayed stable but significantly lower phosphate levels, with values of 50 µmol/L recorded in both April and October. These results are affirmed using Fig. 1b and c as Last Chance Lake contains considerably more phosphate than Goodenough Lake (Tutolo et al. 2024). This result is consistent with microbial studies of GE, where nutrient levels are kept low due to intense biological cycling (Haas et al. 2024).

The Basque Lakes system demonstrated distinct variability in phosphate concentrations across individual lakes. Basque Lake 4 (BL4) exhibited the widest seasonal range, from negligible levels of 1 µmol/L in April to 200 µmol/L in October. In contrast, Basque Lake 1 (BL1) maintained relatively stable but higher phosphate levels, increasing slightly from 140 µmol/L in April to 170 µmol/L in October. Basque Lake 3 (BL3) remained constant at 30 µmol/L. Two samples taken in adjacent pools during April 2024 had phosphate concentrations of 20 µmol/L and 1 µmol/L. Basque Lake 2 (BL2) analyses are not presented in this results section due to the nature of the lake. As pictured in Figure 6, this lake is composed of many small pools within the larger basin, each with their own unique chemical composition. The diverse composition between individual pools in this lake system led to difficulties in analysis and therefore has resulted in a lack of presentable results for BL2.

3.1.2 Chloride as a Tracer in Soda Lakes

Chloride (Cl^-) concentrations reveal contrasting evaporation behaviors between the lake systems. In LC and GE, chloride concentrations increased significantly from April to October. LC showed a dramatic rise, from 26 mmol/L in April to 160 mmol/L in October, consistent with evaporative concentration. GE displayed a similar trend, with chloride levels increasing from 22 mmol/L in April to 70 mmol/L in October. The strong correlation between chloride and phosphate concentrations in LC supports its use as a conservative tracer in highly evaporative soda lakes (Haas et al. 2024).

However, in the Basque Lakes, chloride did not show a consistent relationship with phosphate or seasonal evaporation. For instance, BL4's chloride concentration decreased slightly from 20 mmol/L in April to 14 mmol/L in October, while BL1 exhibited a more pronounced rise from 28 mmol/L to 65 mmol/L over the same period. BL3 showed only a modest seasonal change, with chloride concentrations declining from 92 mmol/L in April to 79 mmol/L in October. These irregular patterns suggest that chloride may be influenced by additional processes, such as rewetting which can occur in October (Fig. 3a).

3.1.3 Divalent Ion Distribution

The uniquely high magnesium, calcium and sulfate concentrations in the Basque Lakes (Table 1) demonstrate the dominance of divalent ions in the chemistry of these lakes, which not only distinguishes them from other hypersaline systems, but also positions them as analogues for sulfate-dominated brines on Mars and other planetary bodies. Unlike LC and GE, where evaporative processes leads to high concentrations of sodium, which is mostly charge balanced by carbonate alkalinity, the Basque Lakes' geochemistry is dominated by the precipitation and cycling of magnesium, which is mostly charge balanced by sulfate, highlighting their distinct biogeochemical environment.

3.1.4 Alkalinity, Salinity and pH Characteristics

The Basque Lakes (BL) are characterized by exceptionally high magnesium (Mg^{2+}) and sulfate (SO_4^{2-}) concentrations, distinguishing them from the other studied lakes. Magnesium concentrations in BL4 were 1400 mmol/L in October 2022, more than double its April

concentration of 670 mmol/L. Similarly, sulfate levels in BL4 increased markedly from 1100 mmol/L in April to 1800 mmol/L in October, consistent with evaporative concentration. In BL1, magnesium levels exhibited a slight decline from 1000 mmol/L in April to 940 mmol/L in October, while sulfate concentrations remained relatively constant but high, increasing slightly from 1800 mmol/L to 2000 mmol/L. BL3 demonstrated an opposite trend to BL1 with Mg^{2+} concentrations remaining stable, but increasing slightly, from April to October (1300 mmol/L to 1600 mmol/L) and SO_4^{2-} declined slightly over the same period (2300 mmol/L to 2000 mmol/L).

In contrast, LC and GE showed much lower magnesium and sulfate concentrations. LC's magnesium levels increased modestly from 340 µmol/L in April to 1.8 mmol/L in October, with sulfate rising from 29 mmol/L to 84 mmol/L over the same period. GE displayed similar trends, with magnesium increasing from 1.1 mmol/L in April to 3.4 mmol/L in October, and sulfate levels rising from 6 mmol/L to 20 mmol/L. Calcium concentrations also differed markedly between lakes. The Basque Lakes maintained relatively high calcium concentrations (7.3 mmol/L to 20 mmol/L), while LC and GE showed consistently low values (30 µmol/L to 290 µmol/L).

Salinity calculations based on major ion concentrations (Na^+, K^+, Mg^{2+}, Ca^{2+}, Cl^-, SO_4^{2-}, PO_4^{3-}) demonstrate that all studied lakes are saline to hypersaline systems. The Basque Lakes exhibit the highest salinities, with BL3 showing approximately 222 Practical Salinity Units (PSU), followed by BL1 (173 PSU), BL2 (122 PSU), and BL4 (112 PSU), largely driven by their exceptional magnesium and sulfate concentrations. Last Chance Lake and Goodenough Lake, while lower in total salinity, still qualify as saline systems with LC ranging from 13-34 PSU and GE from 6-15 PSU in April 2024. These values reflect the considerable dissolved ion content of these lakes, though the dominant ions differ markedly between the Basque Lakes and the soda lakes, as evidenced by their distinct chemical compositions.

Measured alkalinity and pH are in stark contrast between the soda lakes (Last Chance Lake and Goodenough Lake) and the magnesium-sulfate Basque Lakes. LC displayed the highest alkalinity, consistent with its classification as a soda lake. Alkalinity increased markedly from 0.40 eq/L in April to 1.18 eq/L in October, reflecting evaporative concentration of dissolved inorganic carbon over the summer months. The pH of Last Chance Lake also remained consistently high, decreasing slightly from 10.2 in April to 9.2 in October, suggesting minor buffering effects despite significant evaporative changes. Goodenough Lake similarly demonstrated an alkaline condition, with

alkalinity rising significantly from 0.13 eq/L in April to 0.80 eq/L in October. Its pH remained stable at approximately 10.3 across both seasons, indicative of its buffered alkaline system driven by dissolved carbonate species, particularly CO_3^{2-}.

In contrast, the Basque Lakes exhibited substantially lower alkalinity and more varied pH levels. Across all Basque Lakes, alkalinity remained below 0.1 eq/L, highlighting their non-alkaline nature. BL4 showed negligible changes in alkalinity, maintaining consistent values of 0.01 eq/L across seasons, while BL1 and BL3 displayed only minor fluctuations, with values not exceeding 0.1 eq/L. The consistently low alkalinity within the Basque Lakes supports the low phosphate concentrations within these lakes as the low alkalinity limits phosphate solubility. The pH of the Basque Lakes varied more widely, with BL4 decreasing sharply from 9.2 in April to 7.5 in October. BL1 and BL3 exhibited slightly basic conditions, with pH values remaining below 8.0 across both seasons.

The marked differences in alkalinity and pH between LC/GE and the Basque Lakes reinforce the difference in geochemical regimes of these systems. LC and GE, as classic soda lakes, are dominated by bicarbonate and carbonate buffering, while the Basque Lakes reflect a divalent cation-rich environment with limited buffering capacity.

3.2 Water Isotopic Composition

The isotopic composition of water across the studied lakes reveals significant spatial and temporal variability, reflecting the combined influence of evaporation, precipitation, and hydrological inputs. $\delta^{18}O_{H_2O}$ and $\delta^{2}H_{H_2O}$ values provide critical insights into these processes, as they deviate from the meteoric water baselines established by the Global Meteoric Water Line (GMWL) (Craig 1961) and the regional variant Okanagan Meteoric Water Line (OMWL) (Wassenaar 2011) (Fig. 10). Regional precipitation in this area typically falls between $\delta^{18}O_{H_2O}$ values of -15 ‰ and -17 ‰ as precipitation becomes progressively depleted in heavy isotopes with distance from coastal sources. The complete isotopic dataset for water ($\delta^{18}O_{H_2O}$ and $\delta^{2}H_{H_2O}$) and phosphate ($\delta^{18}O_{PO_4}$) across all sampling periods is presented in Table 2.

Table 2: Isotopic Data of Lake Water Samples and of Dissolved Phosphate

Sample ID	$\delta^{18}O_{H_2O}$ (‰)	$\delta^{2}H_{H_2O}$ (‰)	$\delta^{18}O_{PO_4}$ (‰)
BL3 Oct, 22	0.0	-47	13.8
BL4 Oct, 22	-8.5	-80	13.0
GE Oct, 22	-1.4	-60	-
GE Apr, 23	-7.4	-88	14.8
LC Apr, 23	-14.6	-128	13.8
LC Apr, 23	-14.3	-127	6.9
BL1 Oct, 23	-7.0	-82	15.6
LC Oct, 23	-4.4	-66	16.3
LC Dec, 23	-5.6	-84	14.7
BL1 Apr, 24	-1.4	-69	15.1
BL2 Apr, 24	0.5	-60	16.2
BL3 Apr, 24	-1.3	-65	18.0
BL4, Apr, 24	0.4	-61	17.0
GE Apr, 24	-5.9	-82	16.3
LC Apr, 24	-6.6	-87	15.1
LC Jun, 18	-2.9	-77	-
LC Jun, 18	-2.6	-75	-
LC Jun, 18	-3.0	-80	-
GE Jun, 18	-7.3	-92	-
GE Jun, 18	-6.4	-92	-
GE Jun, 18	-6.7	-94	-
GE Jun, 18	-4.4	-79	-
GE Jun, 18	-6.0	-88	-
GE Jun, 18	-6.5	-89	-
LC Oct, 19	-5.5	-86	-
LC Oct, 19	-7.0	-97	-
LC Oct, 19	-5.6	-90	-
LC Oct, 19	-12.3	-118	-
LC Oct, 19	-5.4	-79	-
GE Oct, 19	-4.7	-77	-
GE Oct, 19	-4.2	-97	-

The comparison of lake isotopic signatures to these meteoric water lines in Figure 10 provides a framework to evaluate the effects of evaporation and local hydrological influences.

It is possible for precipitation events to occur in this region during October (Fig. 3a) contributing water that is isotopically lighter than the heavily evaporated waters present in summer. This precipitation input is particularly evident in the isotopic behavior of certain lakes, as discussed below.

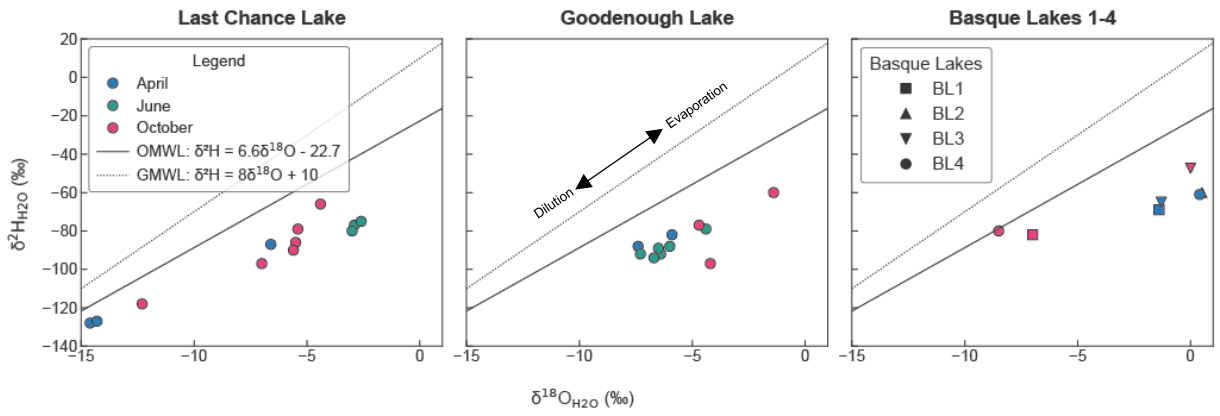

Figure 10: Comparison of $\delta^2H_{H_2O}$ versus $\delta^{18}O_{H_2O}$ values for Last Chance Lake, Goodenough Lake, and Basque Lakes 1–4 against the Global Meteoric Water Line (GMWL) and the Local Meteoric Water Line (OMWL). Data points are color-coded by sampling month (April, June, and October) for Last Chance and Goodenough Lakes, and individual Basque Lakes are distinguished by symbols. Points plotted higher on the plot have undergone greater isotopic depletion in the lighter isotopes of water due to evaporation.

Last Chance Lake exhibited the largest seasonal range in isotopic composition (Table 2), indicative of evaporative enrichment during the October sampling period. $\delta^{18}O_{H_2O}$ values increased from -14.6 ‰ in April to -2.6 ‰ in June, reflecting extreme evaporative isotopic enrichment, before decreasing slightly to -5.6 ‰ in October. Corresponding $\delta^2H_{H_2O}$ values shifted from -128 ‰ in April to -75 ‰ in June and subsequently increased to -66 ‰ in October. This isotopic shift in October reflects an influx of water from precipitation, which is isotopically enriched in the light isotope, ^{16}O, relative to the extremely evaporated waters present in Last Chance Lake during June. The pronounced changes in Last Chance Lake's isotopic composition demonstrate its hypersaline and closed-basin nature, where evaporation dominates during summer, and rewetting events can alter the isotopic signature in fall.

Goodenough Lake demonstrated less pronounced isotopic variability compared to Last Chance Lake, consistent with its less extreme evaporative effects (Table 1). Values of $\delta^{18}O_{H_2O}$ ranged from -7.4 ‰ in April to -4.4 ‰ in June, with further enrichment to -1.4 ‰ in October. Similarly, $\delta^2H_{H_2O}$ values increased from -82 ‰ in April to -79 ‰ in June and then to -60 ‰ in October. These moderate shifts reflect a balance between evaporation and precipitation inputs, with the lake retaining a greater proportion of its water volume compared to Last Chance Lake. The smaller

isotopic shifts between April, June, and October suggest that seasonal changes have a less pronounced effect on water balance at Goodenough Lake.

The Basque Lakes displayed diverse isotopic behavior across individual basins, highlighting the varying hydrological processes within this system. $\delta^{18}O_{H_2O}$ values in BL1 ranged from -1.4 ‰ in April to -7.0 ‰ in October, with $\delta^{2}H_{H_2O}$ values shifting from -69 ‰ to -82 ‰ over this same period. Notably, the October sample was isotopically lighter than the April sample, indicating a precipitation event occurred diluting the lake water with isotopically lighter inputs. BL4 displayed a similar response, with the October sample plotting directly on the OMWL, suggesting significant input from meteoric water during a precipitation event. $\delta^{18}O_{H_2O}$ and $\delta^{2}H_{H_2O}$ values shifted from 0.4 ‰ and -61 ‰ in April to -8.5 ‰ and -80 ‰ in October, reflecting the isotopic influence of the rewetting event on this basin. BL3 exhibited less pronounced isotopic changes compared to BL1 and BL4, perhaps due to its greater water volume, which could dampen the mixing effects of meteoric water input. $\delta^{18}O_{H_2O}$values shifted from -1.3 ‰ in April to 0.0 ‰ in October, with $\delta^{2}H_{H_2O}$ values moving from -65 ‰ to -47 ‰. These moderate changes suggest that BL3 is less sensitive to seasonal precipitation and evaporation than the other Basque Lakes.

The isotopic evolution of water within these lakes demonstrates substantial variability, even between lakes near one another. The extreme shifts in LC reflect its hypersaline, evaporative nature, while the moderate behavior of GE and BL3 points to a greater balance between inflow and evaporation. In contrast, the unexpected isotopic decreases of BL1 and BL4 sometime between April and October provides clear evidence of precipitation events influencing these systems.

3.3 Oxygen Isotopes of Phosphate

A total of fourteen samples successfully underwent silver phosphate precipitation for $\delta^{18}O_{PO_4}$analysis, revealing variability across the three lake systems (Table 2). The standard deviation across 14 samples was 2.63 ‰. LC, a biologically limited system, exhibited the broadest range in $\delta^{18}O_{PO_4}$values ranging from 6.9 ‰ to 16.3 ‰, with the highest value observed in the October sample. A potential analytical error was encountered during the precipitation of a Last Chance Lake sample from April 2023 with a $\delta^{18}O_{PO_4}$ of 13.8 ‰. This data point will be considered an outlier due to the irregularity of it regarding the expected equilibrium $\delta^{18}O_{PO_4}$ of this sample.

In Goodenough Lake, where extensive cyanobacterial mats dominate the margins of the system, $\delta^{18}O_{PO_4}$ values were more consistent, ranging from 14.8 ‰ to 16.3 ‰. This narrower range suggests relatively stable conditions for phosphate cycling compared to Last Chance Lake.

The Basque Lakes (BL1-4) displayed a broad range of $\delta^{18}O_{PO_4}$ values, spanning from 13.0 ‰ to 18.0 ‰. Among the Basque Lakes, BL3 and BL4 exhibited the lowest $\delta^{18}O_{PO_4}$ values, particularly in the October samples. In contrast, BL1 displayed $\delta^{18}O_{PO_4}$ values closer to the higher end of the range regardless of the season.

Methodological testing revealed that silver oxide coating formation through oxidation did not significantly alter $\delta^{18}O_{PO_4}$ values of the final precipitate (Table 3). However, when silver phosphate precipitation occurred in multiple stages, significant isotopic variations were observed between precipitation events from the same sample (Table 3). In other words, incomplete precipitations skew results in favor of lower $\delta^{18}O_{PO_4}$ values, which presumably occurs due to kinetic control on the precipitation reaction. Overall, sample oxidation does not appear to compromise isotopic integrity, but incomplete precipitation does. Quantitative precipitation and/or complete homogenization of multiple precipitates from a single sample is required to avoid unwanted fractionation effects during this step.

Table 3: Fractionation effects observed during sequential precipitation of silver phosphate (Ag_3PO_4) from $\delta^{18}O_{PO_4}$ measurements and photooxidation experiments. The first section of the table compares $\delta^{18}O_{PO_4}$ values for the same sample (LC Apr, 24) precipitated in three stages. The second section reports $\delta^{18}O_{PO_4}$ changes in two different samples subjected to 1-hour and 24-hour photooxidation exposure.

Sample ID	Whole $\delta^{18}O_{PO_4}$ (‰)	1st Precipitation (‰)	2nd Precipitation (‰)	3rd Precipitation (‰)
Values below from 1st, 2nd, and 3rd precipitations of the same sample to determine fractionating effect associated with precipitation of Ag_3PO_4.				
LC Apr, 24	15.1	12.8	15.6	17.2
Values below are from exposing Ag_3PO_4 precipitate from two different samples to photooxidation for 1 hour and 24 hours.				
	Whole $\delta^{18}O_{PO_4}$ (‰)	1 Hour Oxidation (‰)	24 Hour Oxidation (‰)	-
LC Oct, 23	16.3	16.9	16.6	-
LC Oct, 23	16.3	16.5	16.4	-
LC Dec, 23	14.7	14.6	15.0	-
LC Dec, 23	14.7	14.5	14.6	-

3.4 Relationship Between $\delta^{18}O_{PO_4}$ and $\delta^{18}O_{H_2O}$

The relationship between $\delta^{18}O_{PO_4}$ and $\delta^{18}O_{H_2O}$ across the lake systems was evaluated to explore potential connections between phosphate oxygen isotopes and the oxygen isotopic composition of lake water (Fig. 11). Given the limited dataset and the potential for non-linear relationships, Spearman's rank correlation coefficient was calculated to assess the monotonic relationship between $\delta^{18}O_{PO_4}$ and $\delta^{18}O_{H_2O}$. This method is ideal for the study's limited dataset as it is non-parametric and does not require assumptions of normality or linearity. The analysis was performed using the SciPy library in Python, which provides a robust implementation of Spearman's test.

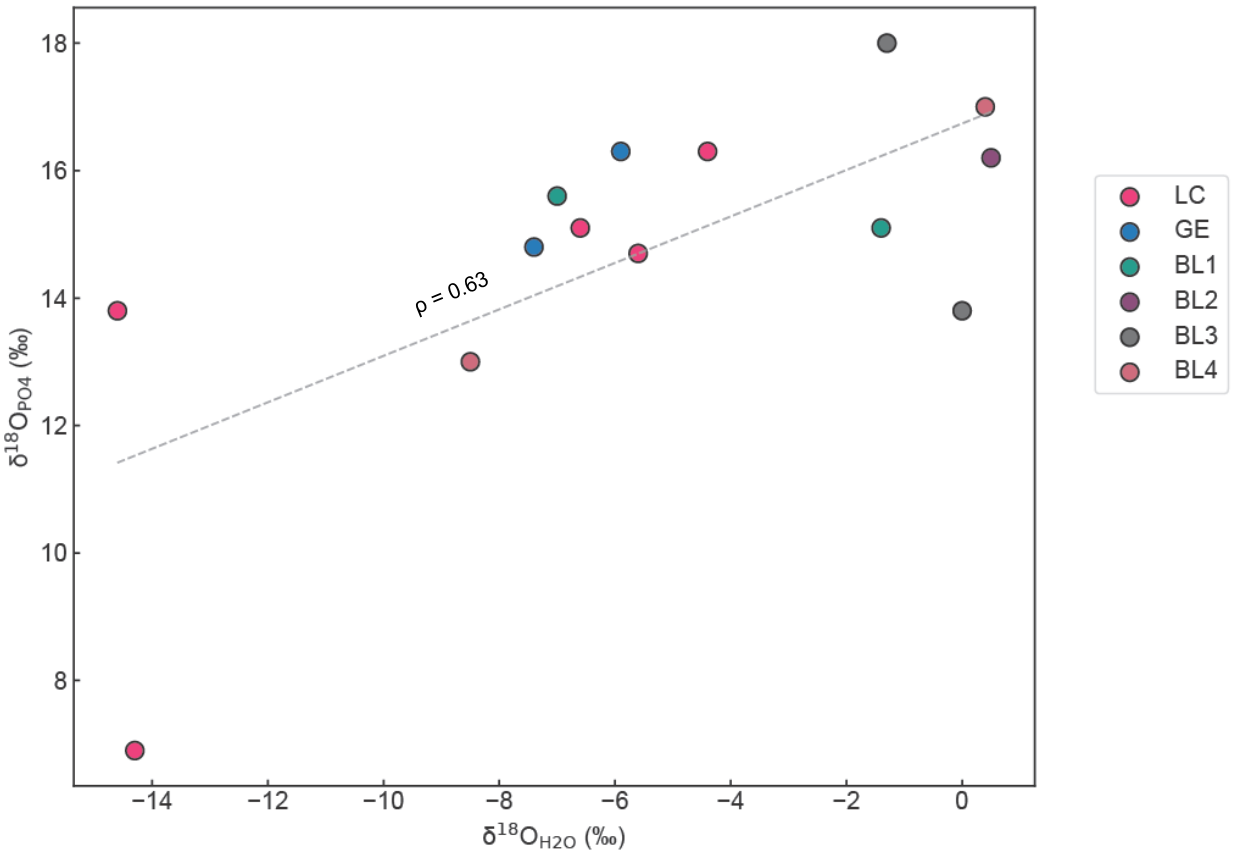

Figure 11: Relationship between δ¹⁸O values of water ($\delta^{18}O_{H_2O}$) and phosphate ($\delta^{18}O_{PO_4}$) across various lake samples. Points are color-coded by sample type, with a regression line (dashed gray) indicating the general trend. The Spearman correlation coefficient (ρ = 0.63) demonstrates a moderate positive correlation between the $\delta^{18}O_{H_2O}$ and $\delta^{18}O_{PO_4}$.

The results of the Spearman's rank correlation test showed a coefficient (ρ) of 0.63, with a p-value < 0.05, indicating a moderate, statistically significant monotonic relationship between $\delta^{18}O_{PO_4}$ and $\delta^{18}O_{H_2O}$. This correlation supports the hypothesis that the isotopic composition of lake water influences the isotopic signature of phosphate, consistent with the interaction between water and phosphate reservoirs during geochemical cycling, but the effects are muted due to the lack of biological cycling in most of these systems. Figure 11 illustrates this relationship, where $\delta^{18}O_{PO_4}$ values increase with $\delta^{18}O_{H_2O}$ across Last Chance, Goodenough, and the Basque Lakes (BL1-4). In Last Chance Lake, the $\delta^{18}O_{PO_4}$ values range from 6.9 ‰ to 16.3 ‰ and align well with the elevated $\delta^{18}O_{H_2O}$ values observed during periods of strong evaporative concentration. Similarly,

GE displays $\delta^{18}O_{PO_4}$ values from 14.8 ‰ to 16.3 ‰, which correspond to its narrower range of $\delta^{18}O_{H_2O}$, reflecting its more moderated hydrological conditions. The Basque Lakes show a broad variability, with $\delta^{18}O_{PO_4}$ values spanning 13.0 ‰ to 18.0 ‰, likely reflecting the distinct isotopic behaviors of BL1-4.

3.5 Expected Equilibrium of $\delta^{18}O_{PO_4}$ ($\delta^{18}O_{PO_4EQ}$)

To assess whether the dissolved phosphate in the studied lakes is in isotopic equilibrium with the surrounding water, the equilibrium equation (7) developed by Chang and Blake (2015) was applied. This equation predicts equilibrium $\delta^{18}O_{PO_4}$ values based on temperature-dependent fractionation effects and the isotopic composition of the surrounding water. To quantify deviations from equilibrium, $\Delta\delta^{18}O_{PO_4}$ was calculated (Eq. 8) and displayed (Fig. 12). Data visualization and statistical analyses were performed using Python, utilizing the pandas library for data manipulation and the matplotlib library for plotting. The dataset was prepared by calculating the difference between expected ($\delta^{18}O_{PO_4EQ}$) and measured values ($\delta^{18}O_{PO_4\,Measured}$). To represent variability across plausible environmental conditions, an error bar of ±1.6 ‰ was displayed, corresponding to the isotopic fractionation range expected over a 1–10°C temperature range, typical of the studied systems. This approach enabled the results to be contextualized across potential equilibrium conditions, highlighting the observed isotopic disequilibrium.

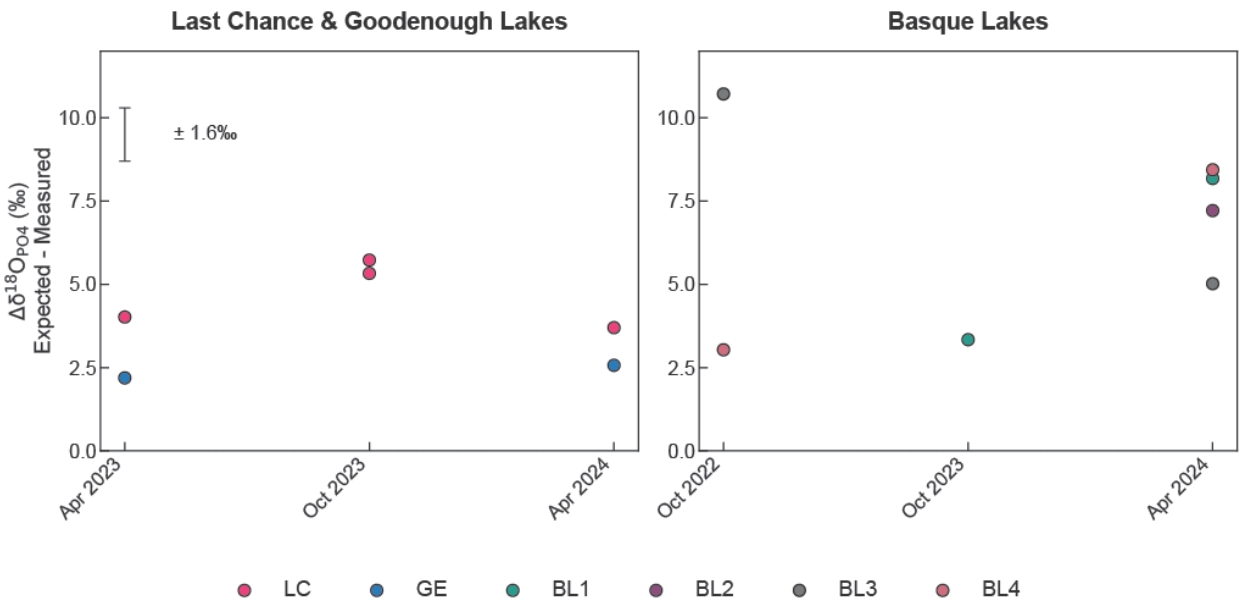

Figure 12: This figure shows the $\Delta\delta^{18}O_{PO_4}$ values for the sampled lakes. Zero represents equilibrium between $\delta^{18}O_{H_2O}$ and $\delta^{18}O_{PO_4}$, with all data points demonstrating a state of disequilibrium that cannot be explained by temperature effects alone. The ±1.6 ‰ error, calculated over a 10°C range, is shown for reference.

Last Chance Lake exhibited significant positive deviations from equilibrium across sampling periods. In April, $\delta^{18}O_{H_2O}$ was -6.6 ‰, and $\delta^{18}O_{PO_4}$ was 15.1 ‰, resulting in a $\Delta\delta^{18}O_{PO_4}$ of +3.7 ‰. By October, $\delta^{18}O_{H_2O}$ increased to -4.4 ‰, and $\delta^{18}O_{PO_4}$ rose to 16.3 ‰, increasing $\Delta\delta^{18}O_{PO_4}$ to +5.3 ‰. This represents a change of +1.6 ‰ shift in disequilibrium between April and October.

Relative to Last Chance, Goodenough Lake displayed small deviations from equilibrium. In April, $\delta^{18}O_{H_2O}$ was -5.9 ‰, and $\delta^{18}O_{PO_4}$ was 16.3 ‰, yielding a $\Delta\delta^{18}O_{PO_4}$ of +2.6 ‰. In October, $\delta^{18}O_{H_2O}$ was -7.4 ‰ and $\delta^{18}O_{PO_4}$ was 14.8 ‰, resulting in a $\Delta\delta^{18}O_{PO_4}$ of +2.2 ‰, which is essentially the same when factoring in uncertainty.

The Basque Lakes exhibited substantial variability in $\Delta\delta^{18}O_{PO_4}$. BL1 had a $\delta^{18}O_{H_2O}$ of -1.4 ‰ and a $\delta^{18}O_{PO_4}$ of 15.1 ‰ in April, resulting in a $\Delta\delta^{18}O_{PO_4}$ of +8.2 ‰. By October, $\delta^{18}O_{H_2O}$ decreased to -7.0, and $\delta^{18}O_{PO_4}$ increased to 15.6 ‰, reducing $\Delta\delta^{18}O_{PO_4}$ to +3.3 ‰. This represents a decrease of -4.9 ‰ in disequilibrium between April and October. BL2, sampled only in April, had a $\delta^{18}O_{H_2O}$ of 0.5 ‰ and a $\delta^{18}O_{PO_4}$ of 16.2 ‰, resulting in a $\Delta\delta^{18}O_{PO_4}$ of +7.2 ‰. BL3 showed

a $\delta^{18}O_{H_2O}$ of -1.3 ‰ and a $\delta^{18}O_{PO_4}$ of 18.0 ‰ in April, yielding a $\Delta\delta^{18}O_{PO_4}$ of +5.0 ‰. In October, $\delta^{18}O_{H_2O}$ was 0.0 ‰, and $\delta^{18}O_{PO_4}$ was 13.8 ‰, with $\Delta\delta^{18}O_{PO_4}$ increasing to +10.7 ‰. This change reflects an increase of +5.7 ‰ in disequilibrium between April and October. BL4 also displayed dynamic patterns, with $\delta^{18}O_{H_2O}$ at 0.4 ‰ and $\delta^{18}O_{PO_4}$ at 17.0 ‰ in April, resulting in a $\Delta\delta^{18}O_{PO_4}$ of +8.4 ‰. By October $\delta^{18}O_{H_2O}$ decreased significantly to -8.5 ‰, while $\delta^{18}O_{PO_4}$ dropped to 13.0 ‰, reducing $\Delta\delta^{18}O_{PO_4}$ to +3.0 ‰. This represents a substantial reduction in disequilibrium of -5.4 ‰ between April and October.

4. Discussion

4.1 Isotopic Signatures and Methodological Advances

The development of reliable analytical methods for measuring $\delta^{18}O_{PO_4}$ in extreme environments presents challenges that have historically limited our understanding of phosphate cycling in prebiotic-analog conditions (McLaughlin et al. 2004; Davies et al. 2014). Traditional protocols face significant matrix effects in highly concentrated solutions, where multiple ion interferences and complex pH dynamics can compromise silver phosphate precipitation (Blake et al. 1997, 2005). This method—modified from Tamburini et al. (2010)—successfully addresses these challenges through specific refinements to precipitation steps, particularly critical for waters with high alkalinity and salinity.

The method's effectiveness is demonstrated by reproducible measurements across dramatically different chemical matrices. In Last Chance Lake, where carbonate alkalinity reaches its peak and salinity exceeds 13 times that of seawater, I obtained consistent $\delta^{18}O_{PO_4}$ measurements ranging from +6.9 ‰ to +16.3 ‰. Similarly, in the magnesium-sulfate dominated Basque Lakes, where divalent ion concentrations approach 2 M, I obtained $\delta^{18}O_{PO_4}$ values from +13.0 ‰ to +18.0 ‰. These measurements span nearly the full range observed in terrestrial systems (Davies et al., 2014), validating the method's applicability across chemical gradients.

Critical methodological advances include modified approaches to chloride removal and precise pH control during precipitation steps. The challenge of chloride interference, particularly severe in Cl-type hypersaline systems, was addressed through iterative pH adjustments and selective

precipitation. This approach allows for separation of silver chloride while preserving phosphate in solution, a crucial improvement for analyzing samples with extremely high Cl^- concentrations. Additionally, careful pH monitoring during precipitation steps ensures complete phosphate recovery while minimizing contamination from other oxygen-bearing compounds.

This methodological advance is particularly significant for origin-of-life studies as it enables investigation of phosphate cycling in environments more representative of potential prebiotic conditions than previously studied systems (Young et al. 2009). The ability to measure $\delta^{18}O_{PO_4}$ in carbonate-rich alkaline and hypersaline conditions provides crucial tools for understanding phosphate behavior in settings where concentrations can reach levels compatible with prebiotic chemistry (Toner and Catling 2020). This capability becomes especially relevant given recent discoveries of similar chemical conditions in extraterrestrial environments (Postberg et al. 2023).

4.2 Lake System Comparisons and Phosphate Dynamics

Together, the studied lakes present a natural laboratory for understanding how fine-scale differences in environmental conditions can significantly alter phosphate cycling in extreme environments. The contrasts in phosphate dynamics between these systems illuminate critical factors controlling both concentration mechanisms and biological utilization, reflecting patterns observed by Blake et al. (2005), who demonstrated how the absence of enzymatic activity drives phosphate isotope disequilibrium in aquatic environments. Importantly, while Chang and Blake (2015) highlighted the role of temperature in phosphate oxygen isotope exchange in natural waters, I stress the importance of micro-environmental factors and seasonal dynamics in sites of origin-of-life and/or astrobiological significance.

4.2.1 Last Chance Lake

Last Chance Lake demonstrates how specific geochemical conditions, such as carbonate-induced calcium removal, can maintain phosphate at concentrations orders of magnitude higher than typical environmental levels (Hudson et al. 2000; Toner and Catling 2020). The lake's significant deviations from isotopic equilibrium ($\Delta\delta^{18}O_{PO_4}$ up to +5.3 ‰, Fig. 12) during periods of high evaporative concentration of dissolved ions suggest minimal biological mediation of the widely

available phosphate pool. This observation aligns with findings from Blake et al. (2005), who reported how enzymatic activity is critical in driving phosphate cycling toward isotopic equilibrium. However, in an environment like Last Chance Lake, where salinity and nitrogen limitation appear to inhibit overall microbial activity (Haas et al. 2024), these pathways may remain inactive. This leads to $\delta^{18}O_{PO_4}$ values that mirror abiotic patterns in extreme chemical conditions, as described by Jaisi et al. (2010). It has also been suggested that extreme oceanic conditions in the Archean eon (4.0-2.5 billion years ago) may have suppressed biological cycling, creating environments where geochemical processes dominate and $\delta^{18}O_{PO_4}$ deviates significantly from equilibrium values (Blake et al. 2010).

When considering all the lakes in this study, the importance of deviation from isotopic equilibrium is further supported by the broad, moderate correlation between $\delta^{18}O_{PO_4}$ and $\delta^{18}O_{H_2O}$ across all samples (Fig. 11). Phosphate-water exchange, mediated by microbial processing of phosphate, is reflected in a strong positive correlation between the oxygen isotopic ratio within the environmental water and the ratio within the dissolved phosphate molecule (Blake et al. 2001). Herein, this relationship was only moderately correlated ($\rho = 0.63$, Fig. 11), suggesting limited isotopic exchange. Additionally, Chang and Blake (2021) emphasized how, in environments where biological influence is restricted, temperature-driven fractionation governs equilibrium between $\delta^{18}O_{PO_4}$ and $\delta^{18}O_{H_2O}$. The result is longer equilibration in abiotic versus biotic systems. To account for likely variances in temperature in the environment as compared to those measured in the field I conducted the equilibrium calculations across a temperature range of 1-10°C. This yielded an uncertainty of only ±1.6 ‰ in the expected equilibrium values, a relatively small range which makes the observed deviations from equilibrium even more significant, as they cannot be explained by temperature variation alone. Increasing the $\Delta\delta^{18}O_{PO_4}$ data volume for these lake systems—so that an individual correlation could be applied to each lake—would be a positive development in the study of these systems, as it would more clearly test the validity of the results presented here.

4.2.2 Goodenough Lake

Goodenough Lake presents a contrasting image when compared to Last Chance Lake, though both deviate from typical freshwater behavior. Despite identical climate and input chemistry (Tutolo et al. 2024) and similar alkaline conditions, Goodenough Lake maintains much lower phosphate concentrations, at least in part due to more active cycling by extensive cyanobacterial mat communities. The lake's consistent isotopic signatures and minimal deviation from the expected equilibrium ($\Delta\delta^{18}O_{PO_4}$ ~ +2.2–2.6 ‰, Fig. 12) reflect rapid intracellular processing through enzymatic pathways, primarily driven by PPase activity (Blake et al. 2005). Furthermore, the observed equilibrium signatures align with the findings of Chang and Blake (2015), who calibrated equilibrium fractionation factors for phosphate, emphasizing their applicability in biologically active settings. Goodenough Lake displays an evolution in its $\delta^{18}O_{H_2O}$ and $\delta^{2}H_{H_2O}$ signatures that is broadly similar to that observed at Last Chance Lake (Fig. 10) Both lakes exhibit enrichment of ^{2}H and ^{18}O from April to October, because ^{1}H and ^{16}O-containing water molecules are preferentially evaporated (Kendall and Coplen 2001). However, a notable difference emerges between the lakes when considering the heightened magnitude shift in water isotope ratios in Last Chance Lake. Goodenough Lake experiences less extreme isotopic evolution than Last Chance Lake, as evidenced by the tighter clustering of points in the Goodenough subplot of Figure 10 compared to the broader spacing seen in the Last Chance subplot. The evolution of the June samples between the two lakes therefore points to a stronger evaporative effect on Last Chance Lake compared to Goodenough Lake. In sum, both lakes experience significant evaporation that modifies their $\delta^{18}O_{H_2O}$ and $\delta^{2}H_{H_2O}$ values, but Last Chance Lake appears more susceptible to evaporative enrichment of ^{18}O. This is likely due to hydrological controls that lead to a stronger net evaporative flux, which is evident in the complete loss of surface water shown in Figure 4. A secondary control on evaporation may be the absence of microbial mat communities at Last Chance Lake. Specifically, the microbial mats in Goodenough Lake could be acting as a cohesive barrier that reduces water loss through evaporation (Schultze-Lam et al., 1996). Such mats can also darken the lake surface, lowering albedo and potentially further restricting evaporation (Schultze-Lam et al., 1996). This biological influence is absent in Last Chance Lake, which may be contributing to the more pronounced isotopic enrichment observed in its waters during June.

4.2.3 The Basque Lakes

The Basque Lakes system provides additional context for understanding phosphate cycling in extreme environments, presenting a third regime where magnesium-sulfate dominated chemistry creates distinct conditions. Each of the Basque Lakes (BL1–4) displays a marked disequilibrium in their $\delta^{18}O_{PO_4}$ signatures (Fig. 12). Notably, BL3 exhibits a persistent and pronounced isotopic disequilibrium ($\Delta\delta^{18}O_{PO_4}$+10.7 ‰), suggesting minimal biological processing akin to Last Chance Lake. However, in BL3, this disequilibrium could be driven by a different biogeochemical mechanism. The combination of limited phosphate availability and prohibitively high concentrations of divalent ions (Table 1) can hinder effective phosphate cycling (Van Dam et al. 2010). This would perpetuate the observed, persistent state of oxygen isotopic disequilibrium between phosphate and water.

BL1 and BL4 are suspected to have experienced meteoric water input sometime near when sampling occurred, as they plot near and/or on the OMWL (Fig. 10). Due to the small and shallow nature of BL1 and BL4, relatively small meteoric inputs could cause water isotopic compositions to shift dramatically. This input would have raised the $\delta^{18}O_{PO_4EQ}$ as outlined in (Eq. 7), thus lowering the equilibrium deviation ($\Delta\delta^{18}O_{PO_4}$) calculated for BL1 and BL4 in October samples. Thus, methods deployed in this thesis may be especially vulnerable to the effects of short-term recharge in evaporative systems, where limited water volumes are poorly buffered against isotopic change via new inputs. High frequency tracking of precipitation events, $\delta^{18}O_{H_2O}$, and $\delta^{18}O_{PO_4}$ would better elucidate the magnitude of this effect.

BL2 exhibits significant spatial heterogeneity, comprising multiple pools within a larger basin, each with distinct isotopic identities. Phosphate concentrations in two adjacent pools differ markedly, at 20 μmol/L and 0.1 μmol/L. Seasonal evaporation further accentuates these differences, as the lake rapidly evaporates within these discrete pools (Fig. 7). Consequently, treating BL2 as a homogeneous system is inappropriate. This scenario parallels the relationship between Last Chance Lake and Goodenough Lake as neighboring water bodies with distinct isotopic signatures and phosphate concentrations. Within BL2, individual basins may serve as comparative environments, highlighting that the search for life or its propagation may not merely involve finding the right environment but identifying specific locales within that environment where minute spatial (in this case, meter-scale) differences play a critical role. This observation

aligns with findings from studies on spatial variability in lake basins, which emphasize the importance of localized conditions on various biogeochemical processes (Zhao et al. 2024).

4.2.4 Synthesis of Lake System Phosphate Cycling Dynamics

The comparative analysis of these saline lake systems reveals distinct phosphate cycling regimes controlled by the interplay of geochemical and biological factors. Last Chance Lake demonstrates how extreme salinity and nitrogen limitation can suppress biological mediation of phosphate cycling, resulting in significant deviations from isotopic equilibrium ($\Delta\delta^{18}O_{PO_4}$ up to +5.3 ‰) despite high phosphate concentrations. In contrast, Goodenough Lake maintains lower phosphate concentrations and near-equilibrium isotopic signatures ($\Delta\delta^{18}O_{PO_4}$ ~ +2.2–2.6 ‰) due to active cycling by microbial communities, despite sharing similar bedrock geology and climate conditions with Last Chance Lake. The Basque Lakes system, particularly BL3, presents a third regime where high divalent ion concentrations create distinct barriers to phosphate cycling, leading to persistent isotopic disequilibrium ($\Delta\delta^{18}O_{PO_4}$ +10.7 ‰). The spatial heterogeneity observed in BL2, with phosphate concentrations varying by two orders of magnitude between adjacent pools (20 µmol/L versus 0.1 µmol/L), further emphasizes how localized conditions can significantly influence phosphate dynamics. Taken together, these findings demonstrate that while geochemical conditions can facilitate phosphate concentration mechanisms, biological activity, when present, plays a dominant role in driving systems toward isotopic equilibrium through enzymatic processing. This relationship between biological activity and isotopic signatures provides a framework for interpreting phosphate cycling in both modern and ancient extreme environments.

4.2.5 Kinetic Modeling Limitations

In their 2021 study, Chang and Blake conducted controlled experiments to determine oxygen isotope exchange rates between phosphate and water catalyzed by PPase. This study used a standardized PPase concentration of 0.16 units per micromole of phosphate across moderate phosphate levels to reasonably constrain and model the exchange rates. However, applying this kinetic model to natural systems, particularly extreme environments like Last Chance Lake, presents challenges. The model's reliance on PPase concentrations and controlled conditions does

not account for the complexities of natural ecosystems, where factors such as nutrient limitations and varying microbial activity significantly influence enzyme availability and activity.

In Last Chance Lake, exceptionally high phosphate concentrations coexist with nitrogen limitation and low overall microbial activity for an alkaline lake (Haas et al. 2024). These conditions hinder the accurate scaling of PPase concentrations relative to those of dissolved phosphate, as assumed in Chang and Blake (2021). Therefore, the persistent disequilibrium observed in $\delta^{18}O_{PO_4}$ values in Last Chance Lake likely reflects these ecological constraints. High salinity and nitrogen limitation apparently restrict microbial activity and, by extension, intracellular phosphate cycling. This contrasts with purely kinetic barriers to oxygen isotope exchange in the experimental setting of Chang and Blake (2021).

My findings suggest that while the first-order kinetic model effectively describes PPase-mediated exchange under controlled conditions, its application to natural systems, especially extreme environments, requires significant refinement. Future research should focus on developing methods to measure PPase activity or concentration directly in situ, enabling more accurate modeling of oxygen isotope exchange rates in systems where nutrient limitations and low microbial activity strongly control phosphate cycling.

4.3 Implications for Prebiotic Chemistry and Astrobiology

The phosphate dynamics observed in these modern analog environments provide critical insights into both origin-of-life studies and potential extraterrestrial biosignatures. Last Chance Lake demonstrates that natural environments can achieve phosphate concentrations compatible with prebiotic chemistry experiments (10-37 mM; Powner et al. 2009; Morasch et al. 2019). The lake's isotopic signatures, characterized by significant deviations from equilibrium ($\delta^{18}O_{PO_4}$ + 3.7 ‰ to +5.3 ‰), establish a baseline for identifying abiotic phosphate accumulation in planetary settings.

The relationship between phosphate cycling and water isotopes in these lakes thus offers a framework for distinguishing biological from abiotic processes in ancient or extraterrestrial environments. The moderate correlation between $\delta^{18}O_{PO_4}$ and $\delta^{18}O_{H_2O}$ ($\rho = 0.63$) demonstrates that even in extreme environments, some degree of isotopic coupling occurs. However, it is notably weaker than in typical biological systems where enzymatic cycling drives strong isotopic coupling

(McLaughlin et al. 2004). This distinction provides a potential proxy for the strength of biological phosphate cycling, including whether phosphate is/was the limiting nutrient, in the geological record or on other planets.

The Basque Lakes system's magnesium sulfate-rich chemistry has specific relevance for Mars, where $MgSO_4$ minerals have been repeatedly identified (Squyres et al., 2004; Gendrin et al., 2005; Chipera et al. 2023). The response of BL1 and BL4 to meteoric inputs demonstrates how environmental perturbations can create apparent changes in biosignatures without actual changes in phosphate processing, a crucial consideration for interpreting similar patterns in Martian lake deposits (Hurowitz et al. 2023).

5. Conclusions

This study provides significant new insights into phosphate cycling in extreme environments relevant to origin of life chemistry and astrobiology through detailed analysis of phosphate oxygen isotopes ($\delta^{18}O_{PO_4}$) and water isotopes ($\delta^{18}O_{H_2O}$) in alkaline and saline lakes. Four key scientific outcomes emerge from this work:

First, Last Chance Lake demonstrates how minimal biological processing leads to both elevated phosphate concentrations (~12 mmol/L) and significant deviations from isotopic equilibrium ($\Delta\delta^{18}O_{PO_4}$ up to +5.3 ‰). These large deviations from equilibrium reflect the absence of microbial mediation, allowing phosphate to accumulate to unusually high concentrations through abiotic processes.

Second, Goodenough Lake, despite sharing similar geochemical conditions with Last Chance Lake, maintains substantially lower phosphate concentrations and near-equilibrium isotopic signatures ($\Delta\delta^{18}O_{PO_4}$ ~ +2.2 ‰). This contrast appears to result from extensive microbial mat communities that actively cycle phosphate through enzymatic processes, having the dual effects of driving the system toward isotopic equilibrium and preventing phosphate accumulation.

Third, the diverse behaviors observed across the Basque Lakes system, particularly their response to meteoric water input, illuminate fundamental aspects of phosphate cycling in magnesium sulfate-rich environments. The large isotopic disequilibrium observed in Basque Lake 3

($\Delta\delta^{18}O_{PO_4}$+10.7 ‰) demonstrates how extreme brine chemistry can maintain phosphate far from equilibrium through abiotic processes, an important consideration for interpreting potential biosignatures in analogous environments on Mars or other habitable bodies.

Fourth, I have established a refined analytical protocol for $\delta^{18}O_{PO_4}$ analysis in hypersaline, alkaline waters. This methodological advance addresses challenges in analyzing phosphate isotopes in extreme environments through innovations in precipitation steps and precise pH control. The protocol's success across dramatically different chemical matrices — from carbonate-rich alkaline waters to magnesium sulfate-dominated brines — demonstrates its broad applicability for studying phosphate cycling in previously challenging environments.

Together, these findings not only confirm my initial hypothesis but also establish a robust framework for using phosphate oxygen isotopes to better understand phosphorus cycling in environments analogous to those that may have hosted the origin of life. My research demonstrates that deviations from isotopic equilibrium can serve as reliable indicators of the relative influence of biological versus abiotic processes in phosphate cycling. This relationship between isotopic signatures and microbial activity provides a valuable tool for interpreting phosphate cycling, enhancing our understanding of environments that could have supported the emergence of life on Earth and potentially elsewhere in the solar system.

6. References

Adu-Gyamfi, J., Pfahler, V., 2022. Oxygen isotopes of inorganic phosphate in environmental samples: Purification and analysis. Springer, Cham

Arai, Y., Sparks, D.L., 2007. Phosphate reaction dynamics in soils and soil components: A multiscale approach. In: Sparks, D.L. (Ed.), Advances in Agronomy, vol. 94. Academic Press, San Diego, pp. 135–179. https://doi.org/10.1016/S0065-2113(06)94003-6

Becker, S., Schneider, C., Okamura, H., et al., 2018. Wet-dry cycles enable the parallel origin of canonical and non-canonical nucleosides by continuous synthesis. Nat. Commun. 9, 517. https://doi.org/10.1038/s41467-017-02639-1

Berg, J.M., Tymoczko, J.L., Stryer, L., 2010. Biochemistry. W.H. Freeman, New York

Bern, C.R., Birdwell, J.E., Jubb, A.M., 2021. Water-rock interaction and the concentrations of major, trace, and rare earth elements in hydrocarbon-associated produced waters of the United States. Environ. Sci. Process. Impacts 23, 1198–1219. https://doi.org/10.1039/d1em00080b

Blake, R.E., Alt, J.C., Martini, A.M., 2001. Oxygen isotope ratios of PO_4: An inorganic indicator of enzymatic activity and P metabolism and a new biomarker in the search for life. Proc. Natl. Acad. Sci. U.S.A. 98, 2148–2153. https://doi.org/10.1073/pnas.051515898

Blake, R.E., Chang, S.J., Lepland, A., 2010. Phosphate oxygen isotopic evidence for a temperate and biologically active Archaean ocean. Nature 464, 1029–1032. https://doi.org/10.1038/nature08952

Blake, R.E., O'Neil, J.R., Garcia, G.A., 1997. Oxygen isotope systematics of biologically mediated reactions of phosphate: I. Microbial degradation of organophosphorus compounds. Geochim. Cosmochim. Acta 61, 4411–4422. https://doi.org/10.1016/S0016-7037(97)00272-X

Blake, R.E., O'Neil, J.R., Surkov, A.V., 2005. Biogeochemical cycling of phosphorus: Insights from oxygen isotope effects of phosphoenzymes. Am. J. Sci. 305, 596–620. https://doi.org/10.2475/ajs.305.6-8.596

Buffo, J.J., Brown, E.K., Pontefract, A., et al., 2022. The bioburden and ionic composition of hypersaline lake ices: Novel habitats on Earth and their astrobiological implications. Astrobiology 22, 962–980. https://doi.org/10.1089/ast.2021.0078

Butlerow, A., 1861. Formation synthétique d'une substance sucrée. C. R. Acad. Sci. 53, 145–147

Campbell, R.B., Tipper, H.W., 1971. Geology of Bonaparte Lake map-area, British Columbia. Geol. Surv. Can., Memoir 363. Information Canada, Ottawa

Chang, S.J., Blake, R.E., 2015. Precise calibration of equilibrium oxygen isotope fractionations between dissolved phosphate and water from 3 to 37°C. Geochim. Cosmochim. Acta 150, 314–329. https://doi.org/10.1016/j.gca.2014.10.030

Chang, S.J., Blake, R.E., Colman, A.S., 2021. Oxygen isotope exchange rates between phosphate

and water catalyzed by inorganic pyrophosphatase: Implications for the biogeochemical cycle of phosphorus. Earth Planet. Sci. Lett. 570, 117071. https://doi.org/10.1016/j.epsl.2021.117071

Chase, J.E., Arizaleta, M.L., Tutolo, B.M., 2021. A series of data-driven hypotheses for inferring biogeochemical conditions in alkaline lakes and their deposits based on the behavior of Mg and SiO_2. Minerals 11, 106. https://doi.org/10.3390/min11020106

Chipera, S.J., Vaniman, D.T., Rampe, E.B., et al., 2023. Mineralogical investigation of Mg-sulfate at the Canaima drill site, Gale Crater, Mars. J. Geophys. Res. Planets 128, e2023JE008041. https://doi.org/10.1029/2023JE008041

Cohen, Z.R., Ding, D., Zhou, L., et al., 2024. Natural soda lakes provide compatible conditions for RNA and membrane function that could have enabled the origin of life. PNAS Nexus 3, pg. e084. https://doi.org/10.1093/pnasnexus/pgae084

Cole, C.V., Innis, G.S., Stewart, J.W.B., 1977. Simulation of phosphorus cycling in semiarid grasslands. Ecology 58, 2–15. https://doi.org/10.2307/1935104

Craig, H., 1961. Isotopic variations in meteoric waters. Science 133, 1702–1703. https://doi.org/10.1126/science.133.3465.1702

Crisler, J.D., Chen, F., Clark, B.C., Schneegurt, M.A., 2019. Cultivation and characterization of the bacterial assemblage of epsomic Basque Lake, BC. Antonie van Leeuwenhoek 112, 1105–1119. https://doi.org/10.1007/s10482-019-01244-0

Cummings, J.M., 1940. Saline and hydromagnesite deposits of British Columbia. Br. Columbia Dep. Mines, Bulletin 1

Darwin, C., 1859. On the Origin of Species by Means of Natural Selection, or the Preservation of Favoured Races in the Struggle for Life. John Murray, London

Dauphas, N., Schauble, E.A., 2016. Mass fractionation laws, mass-independent effects, and isotopic anomalies. Annu. Rev. Earth Planet. Sci. 44, 709–783. https://doi.org/10.1146/annurev-earth-060115-012157

Davies, C.L., Surridge, B.W.J., Gooddy, D.C., 2014. Phosphate oxygen isotopes within aquatic ecosystems: Global data synthesis and future research priorities. Sci. Total Environ. 496, 563–575. https://doi.org/10.1016/j.scitotenv.2014.07.057

Deamer, D., Singaram, S., Rajamani, S., Kompanichenko, V., Guggenheim, S., 2006. Self-assembly processes in the prebiotic environment. Philos. Trans. R. Soc. Lond. B Biol. Sci. 361, 1809–1818. https://doi.org/10.1098/rstb.2006.1905

Dohaney, J.A.M., 2009. Distribution of the Chilcotin Group basalts, British Columbia. M.Sc. thesis, University of British Columbia, Vancouver, 125 pages

Elghobashi-Meinhardt, N., 2024. ATP hydrolysis captured in atomic detail. Nat. Chem. 16, 306–307. https://doi.org/10.1038/s41557-024-01466-4

Elser, J., Haygarth, P., 2021. Phosphorus: Past and future. Oxford University Press, New York

Epstein, S., Buchsbaum, R., Lowenstam, H.A., Urey, H.C., 1953. Revised carbonate-water

isotopic temperature scale. GSA Bull. 64, 1315–1326. https://doi.org/10.1130/0016-7606(1953)64[1315:RCITS]2.0.CO;2

Eugster, H.P., Hardie, L.A., 1978. Saline lakes. In: Lerman, A. (Ed.), Lakes: Chemistry, Geology, Physics. Springer, New York, pp. 237–293. https://doi.org/10.1007/978-1-4757-1152-3_8

Filippelli, G.M., 2008. The global phosphorus cycle: Past, present, and future. Elements 4, 89–95. https://doi.org/10.2113/gselements.4.2.89

Fox-Powell, M.G., Cockell, C.S., 2018. Building a geochemical view of microbial salt tolerance: Halophilic adaptation of Marinococcus in a natural magnesium sulfate brine. Front. Microbiol. 9, 739. https://doi.org/10.3389/fmicb.2018.00739

Fry, B., 2006. Stable Isotope Ecology. Springer, New York

Gat, J.R., 1981. Stable isotope hydrology: Deuterium and oxygen-18 in the water cycle. International Atomic Energy Agency (IAEA), Vienna

Gendrin, A., Mangold, N., Bibring, J.-P., et al., 2005. Sulfates in Martian layered terrains: The OMEGA/Mars Express view. Science 307, 1587–1591. https://doi.org/10.1126/science.1109087

Gislason, S.R., Oelkers, E.H., 2003. Mechanism, rates, and consequences of basaltic glass dissolution: II. An experimental study of the dissolution rates of basaltic glass as a function of pH and temperature. Geochim. Cosmochim. Acta 67, 3817–3832. https://doi.org/10.1016/S0016-7037(03)00176-5

Goudge, M.F., 1926. Investigations of mineral resources and the mining industry. Canada Mines Branch 687, 19–31. https://doi.org/10.1038/149728a0

Greenwood, J.P., Blake, R.E., 2006. Evidence for an acidic ocean on Mars from phosphorus geochemistry of Martian soils and rocks. Geology 34, 953–956. https://doi.org/10.1130/G22415A.1

Haas, S., Sinclair, K.P., Catling, D.C., 2024. Biogeochemical explanations for the world's most phosphate-rich lake, an origin-of-life analog. Commun. Earth Environ. 5, 28. https://doi.org/10.1038/s43247-023-01192-8

Haines, M., Khot, V., Strous, M., 2023. The vigor, futility, and application of microbial element cycles in alkaline soda lakes. Elements 19, 30–36. https://doi.org/10.2138/gselements.19.1.30

Hao, J., Glein, C.R., Huang, F., et al., 2022. Abundant phosphorus expected for possible life in Enceladus's ocean. Proc. Natl. Acad. Sci. U.S.A. 119, e2201388119. https://doi.org/10.1073/pnas.2201388119

Hausrath, E.M., Adcock, C.T., Berger, J.A., et al., 2024. Phosphates on Mars and their importance as igneous, aqueous, and astrobiological indicators. Minerals 14, 591. https://doi.org/10.3390/min14060591

Hirst, J.F., 1995. Sedimentology, diagenesis and hydrochemistry of the saline, alkaline lakes on

the Cariboo Plateau, Interior British Columbia, Canada. M.Sc. thesis, University of Saskatchewan, Saskatoon, 285 pages

Hoefs, J., 2009. Stable Isotope Geochemistry, 6th ed. Springer, Berlin. https://doi.org/10.1007/978-3-540-70708-0

Hudson, J.J., Taylor, W.D., Schindler, D.W., 2000. Phosphate concentrations in lakes. Nature 406, 54–56. https://doi.org/10.1038/35017533

Hurowitz, J.A., Catling, D.C., Fischer, W.W., 2023. High carbonate alkalinity lakes on Mars and their potential role in an origin of life beyond Earth. Elements 19, 37–44. https://doi.org/10.2138/gselements.19.1.37

Ingalls, M., Blättler, C.L., Higgins, J.A., et al., 2020. P/Ca in carbonates as a proxy for alkalinity and phosphate levels. Geophys. Res. Lett. 47, e2020GL088804. https://doi.org/10.1029/2020GL088804

Jaisi, D.P., Blake, R.E., 2014. Advances in using oxygen isotope ratios of phosphate to understand phosphorus cycling in the environment. In: Sparks, D.L. (Ed.), Advances in Agronomy, vol. 125. Academic Press, San Diego, pp. 1–53. https://doi.org/10.1016/B978-0-12-800137-0.00001-4

Jaisi, D.P., Blake, R.E., Kukkadapu, R.K., 2010. Fractionation of oxygen isotopes in phosphate during its interactions with iron oxides. Geochim. Cosmochim. Acta 74, 1309–1319. https://doi.org/10.1016/j.gca.2009.11.010

Jenkins, O.P., 1918. Spotted lakes of epsomite in Washington and British Columbia. Am. J. Sci. 46, 638–644. https://doi.org/10.2475/ajs.s4-46.275.638

Jones, B.F., Naftz, D.L., Spencer, R.J., Oviatt, C.G., 2009. Geochemical evolution of Great Salt Lake, Utah, USA. Aquat. Geochem. 15, 95–121. https://doi.org/10.1007/s10498-008-9047-y

Karl, D.M., Tien, G., 1992. MAGIC: A sensitive and precise method for measuring dissolved phosphorus in aquatic environments. Limnol. Oceanogr. 37, 105–116. https://doi.org/10.4319/lo.1992.37.1.0105

Van Kauwenbergh, S.J., 2010. World phosphate rock reserves and resources. Technical Bulletin IFDC-T-75. International Fertilizer Development Center, Muscle Shoals, AL, 48 pages

Kendall, C., Coplen, T.B., 2001. Distribution of oxygen-18 and deuterium in river waters across the United States. Hydrol. Process. 15, 1363–1393. https://doi.org/10.1002/hyp.217

Kendall, C., McDonnell, J.J. (Eds.), 1998. Isotope Tracers in Catchment Hydrology. Elsevier, Amsterdam

Larsen, S., Middelboe, V., Johansen, H.S., 1989. The fate of ^{18}O-labelled phosphate in soil/plant systems. Plant Soil 117, 143–145. https://doi.org/10.1007/BF02206267

Lécuyer, C., Grandjean, P., Sheppard, S.M.F., 1999. Oxygen isotope exchange between dissolved phosphate and water at temperatures ≤135°C: Inorganic versus biological fractionations. Geochim. Cosmochim. Acta 63, 855–862. https://doi.org/10.1016/S0016-

7037(99)00096-4

Liang, Y., Blake, R.E., 2006a. Oxygen isotope composition of phosphate in organic compounds: Isotope effects of extraction methods. Org. Geochem. 37, 1263–1277. https://doi.org/10.1016/j.orggeochem.2006.03.009

Liang, Y., Blake, R.E., 2006b. Oxygen isotope signature of Pi regeneration from organic compounds by phosphomonoesterases and photooxidation. Geochim. Cosmochim. Acta 70, 3957–3969. https://doi.org/10.1016/j.gca.2006.04.036

Lis, H., Weiner, T., Pitt, F.D., et al., 2019. Phosphate uptake by cyanobacteria is associated with kinetic fractionation of phosphate oxygen isotopes. ACS Earth Space Chem. 3, 233–239. https://doi.org/10.1021/acsearthspacechem.8b00099

Liu, L., Zou, Y., Bhattacharya, A., et al., 2020. Enzyme-free synthesis of natural phospholipids in water. Nat. Chem. 12, 1029–1034. https://doi.org/10.1038/s41557-020-00559-0

Lloyd, R.M., 1964. Variations in the oxygen and carbon isotope ratios of Florida Bay mollusks and their environmental significance. J. Geol. 72, 84–111. https://doi.org/10.1086/626966

Mathews, W.H., 1989. Neogene Chilcotin basalts in south-central British Columbia: Geology, ages, and geomorphic history. Can. J. Earth Sci. 26, 969–982. https://doi.org/10.1139/e89-078

McLaughlin, K., Cade-Menun, B.J., Paytan, A., 2006. The oxygen isotopic composition of phosphate in Elkhorn Slough, California: A tracer for phosphate sources. Estuar. Coast. Shelf Sci. 70, 499–506. https://doi.org/10.1016/j.ecss.2006.06.030

McLaughlin, K., Silva, S., Kendall, C., et al., 2004. A precise method for the analysis of $\delta^{18}O$ of dissolved inorganic phosphate in seawater. Limnol. Oceanogr. Methods 2, 202–212. https://doi.org/10.4319/lom.2004.2.202

Melby, E.S., Soldat, D.J., Barak, P., 2013. Preferential soil sorption of oxygen-18-labeled phosphate. Commun. Soil Sci. Plant Anal. 44, 2371–2377. https://doi.org/10.1080/00103624.2013.800100

Marshall, M., 2020. The water paradox and the origins of life. Nature 588, 210–213. https://doi.org/10.1038/d41586-020-03461-4

Morasch, M., Liu, J., Dirscherl, C.F., et al., 2019. Heated gas bubbles enrich, crystallize, dry, phosphorylate and encapsulate prebiotic molecules. Nat. Chem. 11, 779–788. https://doi.org/10.1038/s41557-019-0299-5

Mouginis-Mark, P.J., Wilson, L., 2022. Terrestrial analogs to planetary volcanic phenomena. In: Oxford Research Encyclopedia of Planetary Science. Oxford University Press. https://doi.org/10.1093/acrefore/9780190647926.013.253

Nesbitt, H.W., 1990. Groundwater evolution, authigenic carbonates, and sulfates, of the Basque Lake No. 2 Basin, Canada. Spec. Publ. Geochem. Soc. Fluid-Miner. Interact. 2, 355–371

Nichols, F., Pontefract, A., Dion-Kirschner, H., et al., 2023. Lipid biosignatures from SO_4-rich hypersaline lakes of the Cariboo Plateau. J. Geophys. Res. Biogeosciences 128,

e2023JG007480. https://doi.org/10.1029/2023JG007480

Oró, J., 1961. Comets and the formation of biochemical compounds on the primitive Earth. Nature 190, 389–390. https://doi.org/10.1038/190389a0

Patel, B.H., Percivalle, C., Ritson, D.J., et al., 2015. Common origins of RNA, protein and lipid precursors in a cyanosulfidic protometabolism. Nat. Chem. 7, 301–307. https://doi.org/10.1038/nchem.2202

Pecoraino, G., D'Alessandro, W., Inguaggiato, S., 2015. The other side of the coin: Geochemistry of alkaline lakes in volcanic areas. In: Rouwet, D., Christenson, B., Tassi, F., Vandemeulebrouck, J. (Eds.), Volcanic Lakes. Springer, Berlin, Heidelberg, pp. 219–237. https://doi.org/10.1007/978-3-662-46300-4_12

Pfahler, V., Connell, D.O., Tamburini, F., 2022. Oxygen isotopes of inorganic phosphate in environmental samples. Springer International Publishing, Cham

Postberg, F., Sekine, Y., Klenner, F., et al., 2023. Detection of phosphates originating from Enceladus's ocean. Nature 618, 489–493. https://doi.org/10.1038/s41586-023-05987-9

Powner, M.W., Gerland, B., Sutherland, J.D., 2009. Synthesis of activated pyrimidine ribonucleotides in prebiotically plausible conditions. Nature 459, 239–242. https://doi.org/10.1038/nature08013

Raudsepp, M.J., Wilson, S., Morgan, B., 2023. Making salt from water: The unique mineralogy of alkaline lakes. Elements 19, 22–29. https://doi.org/10.2138/GSELEMENTS.19.1.22

Raudsepp, M.J., Wilson, S., Zeyen, N., et al., 2024. Magnesite everywhere: Formation of carbonates in the alkaline lakes and playas of the Cariboo Plateau, British Columbia, Canada. Chem. Geol. 648, 121951. https://doi.org/10.1016/j.chemgeo.2024.121951

Reinhard, C.T., Planavsky, N.J., Gill, B.C., et al., 2017. Evolution of the global phosphorus cycle. Nature 541, 386–389. https://doi.org/10.1038/nature20772

Renaut, R.W., 1990. Recent carbonate sedimentation and brine evolution in the saline lake basins of the Cariboo Plateau, British Columbia, Canada. Hydrobiologia 197, 67–81. https://doi.org/10.1007/BF00026939

Renaut, R.W., Long, P.R., 1989. Sedimentology of the saline lakes of the Cariboo Plateau, Interior British Columbia, Canada. Sediment. Geol. 64, 239–264. https://doi.org/10.1016/0037-0738(89)90051-1

Renaut, R.W., Stead, D., 1994. Last Chance Lake, a natric playa-lake in interior British Columbia, Canada. In: Global Geological Record of Lake Basins, pp. 425–427

Rosas, J.C., Korenaga, J., 2021. Archaean seafloors shallowed with age due to radiogenic heating in the mantle. Nat. Geosci. 14, 79–83. https://doi.org/10.1038/s41561-020-00673-1

Rosen, M., 1994. The importance of groundwater in playas: A review of playa classifications and the sedimentology and hydrology of playas. In: Paleoclimate and Basin Evolution of Playa Systems, pp. 1–18

Russell, J.K., Edwards, B.R., Williams-Jones, G., Hickson, C.J., 2023. Pleistocene to Holocene

volcanism in the Canadian Cordillera. Can. J. Earth Sci. 60, 1443–1466. https://doi.org/10.1139/cjes-2023-0065

Ruttenberg, K.C., 2014. The global phosphorus cycle. In: Turekian, K.K., Holland, H.D. (Eds.), Treatise on Geochemistry, 2nd ed. Elsevier, Oxford, pp. 585–643. https://doi.org/10.1016/b978-0-08-095975-7.00813-5

Schultze-Lam, S., Ferris, F.G., Sherwood-Lollar, B., Gerits, J.P., 1996. Ultrastructure and seasonal growth patterns of microbial mats in a temperate climate saline-alkaline lake: Goodenough Lake, British Columbia, Canada. Can. J. Microbiol. 42, 147–161. https://doi.org/10.1139/m96-023

Schwartz, A.W., 2006. Phosphorus in prebiotic chemistry. Philos. Trans. R. Soc. Lond. B Biol. Sci. 361, 1743–1749. https://doi.org/10.1098/rstb.2006.1901

Sharp, Z.D., 2017. Principles of Stable Isotope Geochemistry, 2nd ed. Pearson, Upper Saddle River, NJ

Shen, J., Smith, A.C., Claire, M.W., Zerkle, A.L., 2020. Unraveling biogeochemical phosphorus dynamics in hyperarid Mars-analogue soils using stable oxygen isotopes in phosphate. Geobiology 18, 760–779. https://doi.org/10.1111/gbi.12408

Siegel, F.R., 1961. Factors influencing the precipitation of dolomitic carbonates. Bull. Kansas Geol. Surv. 129–158

Talbot, M.R., 1990. A review of the palaeohydrological interpretation of carbon and oxygen isotopic ratios in primary lacustrine carbonates. Chem. Geol. Isot. Geosci. Sect. 80, 261–279. https://doi.org/10.1016/0168-9622(90)90009-2

Tamburini, F., Bernasconi, S.M., Angert, A., et al., 2010. A method for the analysis of the $\delta^{18}O$ of inorganic phosphate extracted from soils with HCl. Eur. J. Soil Sci. 61, 1025–1032. https://doi.org/10.1111/j.1365-2389.2010.01290.x

Tamburini, F., Pfahler, V., von Sperber, C., et al., 2014. Oxygen isotopes for unraveling phosphorus transformations in the soil–plant system: A review. Soil Sci. Soc. Am. J. 78, 38–46. https://doi.org/10.2136/sssaj2013.05.0186dgs

Toner, J.D., Catling, D.C., 2019. Alkaline lake settings for concentrated prebiotic cyanide and the origin of life. Geochim. Cosmochim. Acta 260, 124–132. https://doi.org/10.1016/j.gca.2019.06.031

Toner, J.D., Catling, D.C., 2020. A carbonate-rich lake solution to the phosphate problem of the origin of life. Proc. Natl. Acad. Sci. U.S.A. 117, 883–888. https://doi.org/10.1073/pnas.1916109117

Tosca, N.J., Tutolo, B.M., 2023. How to make an alkaline lake: Fifty years of chemical divides. Elements 19, 15–21. https://doi.org/10.2138/gselements.19.1.15

Treiman, A.H., Lanza, N.L., VanBommel, S., et al., 2023. Manganese-Iron Phosphate Nodules at the Groken Site, Gale Crater, Mars. Minerals 13, 1122. https://doi.org/10.3390/min13091122

Tribe, S., 2005. Eocene paleo-physiography and drainage directions, southern Interior Plateau, British Columbia. Can. J. Earth Sci. 42, 215–230. https://doi.org/10.1139/e04-062

Tutolo, B.M., Tosca, N.J., 2023. Dry, salty, and habitable: The science of alkaline lakes. Elements 19, 10–14. https://doi.org/10.2138/gselements.19.1.10

Tutolo, BM, R Perrin, R Lauer, S Bossaer, NJ Tosca, S Sevgen, M Nightingale, D Ilg, E Mott, T Wilson (2024) Groundwater-driven evolution of prebiotic alkaline lake environments. *Life* 14 1624

Urey, H.C., 1947. The thermodynamic properties of isotopic substances. J. Chem. Soc. 562–581. https://doi.org/10.1039/jr9470000562

Urey, H.C., 1948. Oxygen isotopes in nature and in the laboratory. Science 108, 489–496. https://doi.org/10.1126/science.108.2810.489

Van Dam, R.A., Hogan, A.C., McCullough, C.D., et al., 2010. Aquatic toxicity of magnesium sulfate, and the influence of calcium, in very low ionic concentration water. Environ. Toxicol. Chem. 29, 410–421. https://doi.org/10.1002/etc.56

Vos, H.M.J., Ros, M.B.H., Koopmans, G.F., van Groenigen, J.W., 2014. Do earthworms affect phosphorus availability to grass? A pot experiment. Soil Biol. Biochem. 79, 34–42. https://doi.org/10.1016/j.soilbio.2014.08.018

Wassenaar, L.I., Athanasopoulos, P., Hendry, M.J., 2011. Isotope hydrology of precipitation, surface, and ground waters in the Okanagan Valley, British Columbia, Canada. J. Hydrol. 411, 37–48. https://doi.org/10.1016/j.jhydrol.2011.09.032

Westheimer, F.H., 1987. Why nature chose phosphates. Science 235, 1173–1178. https://doi.org/10.1126/science.2434996

Williams, W.D., 1996. The largest, highest and lowest lakes of the world: Saline lakes. SIL Proceedings, 1922-2010 26, 61–79. https://doi.org/10.1080/03680770.1995.11900693

Winter, E.R.S., Carlton, M., Briscoe, H.V.A., 1940. The interchange of heavy oxygen between water and inorganic oxy-anions. J. Chem. Soc. 131–138. https://doi.org/10.1039/JR9400000131

Xinping, Z., Lide, T., Jingmiao, L., 2005. Fractionation mechanism of stable isotope in evaporating water body. J. Geogr. Sci. 15, 375–384. https://doi.org/10.1007/BF02837526

Xu, J., Green, N.J., Gibard, C., et al., 2019. Prebiotic phosphorylation of 2-thiouridine provides either nucleotides or DNA building blocks via photoreduction. Nat. Chem. 11, 457–462. https://doi.org/10.1038/s41557-019-0225-x

Zdanowicz, C.M., Zielinski, G.A., Germani, M.S., 1999. Mount Mazama eruption: Calendrical age verified and atmospheric impact assessed. Geology 27, 621–624. https://doi.org/10.1130/0091-7613(1999)027%3C0621:MMECAV%3E2.3.CO;2

Zhao, S., Hermans, M., Niemistö, J., et al., 2024. Stratification controls the magnitude of in-lake phosphorus cycling: Insights from a morphologically complex eutrophic lake. Hydrobiologia. https://doi.org/10.1007/s10750-024-05701-4

Zorz, J.K., Sharp, C., Kleiner, M., Gordon, P.M.K., Pon, R.T., Dong, X., Strous, M., 2019. A shared core microbiome in soda lakes separated by large distances. Nat. Commun. 10, 1–10. https://doi.org/10.1038/s41467-019-12195-5